Pak.j.stat.oper.res. Vol.20 No. 3 2024 pp 489-515 DOI: http://dx.doi.org/10.18187/pjsor.v20i3.4439

Pakistan Journal of Statistics and Operation Research

A Novel Model for Finance and Reliability Applications: Theory, Practices and Financial Peaks Over a Random Threshold Value-at-Risk Analysis

Abdussalam Aljadani[1], Mahmoud M. Mansour[2,3] and Haitham M. Yousof[3]

* Corresponding Author

[1] Department of Management, College of Business Administration in Yanbu, Taibah University, Al-Madinah, Al-Munawarah 41411, Kingdom of Saudi Arabia; ajadani@taibahu.edu.sa
[2] Department of Management Information Systems, Yanbu, Taibah University, Yanbu 46421, Saudi Arabia; mmmansour@taibahu.edu.sa
[3] Department of Statistics, Mathematics and Insurance, Benha University, Egypt; haitham.yousof@fcom.bu.edu.eg

Abstract

In this paper, the authors introduce a new three-parameter lifetime probability distribution known. They thoroughly examine and describe this distribution, providing insights into its characteristics and its suitability for various applications. This newly constructed distribution's density function exhibits characteristics of both symmetry and right-skewness, providing modelling flexibility across a range of datasets. Because of its skewness coefficient, which can take both positive and negative values, a wide range of data asymmetries can be represented. The Marshall-Olkin generated log-logistic distribution's corresponding hazard rate displays a variety of characteristics, including monotonic increase, increasing-constant, constant, upside-down, and monotonic drop. Because of its adaptability, the distribution can successfully capture various risk or failure rate patterns across time. Using a number of techniques, the researchers expand this distribution to the bivariate domain. Its utility in modelling multivariate lifetime data and inter-variable relationships is improved by these extensions. The researchers use the maximum likelihood method to estimate the parameters of the distribution, which ensures reliable and effective parameter estimation from observed data. They carry out an extensive simulation research to analyse biases and mean squared errors in a range of scenarios and sample sizes in order to evaluate the finite behaviour of the maximum likelihood estimators. In real-life and reliability applications, this meticulous methodology aids in evaluating the estimators' precision and dependability. Because it may offer a comprehensive and nuanced knowledge of high financial risks, the Peaks Over a Random Threshold Value-at-Risk (PORT-VaR) study is crucial for evaluating Norwegian fire insurance claims. This financial analysis is given extra consideration.

Key Words: Risk Analysis; Log-logistic model; Peaks Over a Random Threshold; Marshall-Olkin model; Simulations; Estimation; Reliability Applications; Modeling.

1. Introduction

The log-logistic (LL) probability model is well known for being a flexible statistical tool that may be used in many different fields, such as actuarial science, business, biology, economics, engineering, insurance, etc. Its usefulness extends to a wide range of applications, including evaluating Internet traffic patterns, analyzing business size statistics, and modelling income and wealth disparity. First-rate research by Harris (1968) and Atkinson and Harrison (1978) shown that the LL distribution is a useful tool for modelling wealth and income distributions. Its use to model business size data was further upon by Corbellini et al. (2007).

The LL model has been adopted in research such as by, demonstrating its value in reliability and life testing tests. The LL distribution is especially useful for modelling processes where the risk declines with time because of its notable hazard rate function (HZRF), which monotonically decreases over time. Additionally, it is thought of as a model that,

as Chahkandi and Ganjali (2009) explore, describes residual lifespan at advanced ages. Bryson (1974) noted that the LL distribution provides a heavy-tailed modelling technique, in contrast to typical probability distributions like the exponential (exp), Weibull (W), and Gamma (Gam) distributions. Researchers like Durbey (1970) have thoroughly examined its interaction with other distributions, like the Burr XII and Compound Gamma models, offering greater insights into its adaptability and use in a variety of contexts. The continuous random variable $\boldsymbol{y}$ is characterized as following the LL (Lomax) model with a single scale parameter cc if its cumulative-distribution-function (CDF) for $y > 0$ is given by:

$$W_c(y) = 1 - \frac{1}{\left(\frac{1}{c}y + 1\right)^2}, \tag{1}$$

where $c > 0$ is the parameter of scale, respectively. The probability density function (PDF) corresponding to (1) can be obtained through the following formula

$$w_c(y) = 2\frac{1}{c}\frac{1}{\left(\frac{1}{c}y + 1\right)^3}. \tag{2}$$

When modelling survival data, financial losses, or durations where the rate of occurrence declines over time, this approach is especially helpful in situations where variables have big tails. The distribution's scale and form are influenced by the parameter cc, which gives modelling various datasets and phenomena flexibility. Although the LL and Lomax (Lox) distributions are parameterized differently, they are related by their cumulative distribution functions (also known as CDFs) and have comparable shapes, especially as the Lomax model's shape parameter tends to infinity. There is an important theoretical relationship between both distributions that is highlighted by this convergence. Conversely, the LL and Burr Type XII distributions have comparable forms and are used in similar contexts, particularly when modelling severe events and heavy-tailed data. Their link is not as clear-cut as it is in some other pairings of distributions, despite these similarities. Yousof et al. (2018) state that the Marshall-Olkin-generated-G family (MOG-G) class's cumulative distribution function (PDF) is as follows:

$$F_{b,\boldsymbol{a},\underline{\boldsymbol{\varphi}}}(y) = \frac{1 - \left[1 - W_{\underline{\boldsymbol{\varphi}}}(y)\right]^{\boldsymbol{a}}}{1 - \overline{b}\left[1 - W_{\underline{\boldsymbol{\varphi}}}(y)\right]^{\boldsymbol{a}}} | x \in R, \tag{3}$$

where $W_{\underline{\boldsymbol{\varphi}}}(y)$ is the CDF related to the base-line model and $\overline{b} = (1 - b)$. Then, the new PDF based on (3) is derived as

$$f_{b,\boldsymbol{a},\underline{\boldsymbol{\varphi}}}(y) = b\boldsymbol{a}\frac{w_{\underline{\boldsymbol{\varphi}}}(y)\left[1 - W_{\underline{\boldsymbol{\varphi}}}(y)\right]^{\boldsymbol{a}-1}}{\left\{1 - \overline{b}\left[1 - W_{\underline{\boldsymbol{\varphi}}}(y)\right]^{\boldsymbol{a}}\right\}^2} | x \in R. \tag{4}$$

The Marshall-Olkin-generated LL (MOGZLL) CDF is given by

$$F_{\underline{\boldsymbol{\varphi}}}(y) = \frac{1 - \left(\frac{1}{c}y + 1\right)^{-2\boldsymbol{a}}}{1 - \overline{b}\left(\frac{1}{c}y + 1\right)^{-2\boldsymbol{a}}} | x > 0, \tag{5}$$

where $\underline{\boldsymbol{\Psi}} = (b, \boldsymbol{a}, c)$. This work is primarily focused on improving the adaptability of the LL distribution by combining it with a more versatile family of distributions. The identification problem related to the MOGZLL distribution is precisely calculating the model parameters from the data that is observed. This challenge stems from the fact that the parameters may affect the distribution's structure in comparable ways, which may result in trade-offs or correlations between them. As a result, figuring out each parameter exactly from the distribution of observed data becomes difficult. Parameter identification is influenced by a number of factors, including the characteristics of the data under analysis. For instance, precise parameter estimate may be hampered by small sample sizes or constrained data ranges. Depending on the details of the dataset and the methodology selected, various estimating techniques, such as maximum likelihood, method of moments, or Bayesian approaches, may produce variable estimates, each with varying levels of identifiability and accuracy. Researchers often confine parameters' values or establish permanent relationships between them based on existing knowledge or pragmatic considerations in order to increase

identifiability. By using statistical tests to evaluate the MOGZLL distribution's goodness of fit, one can improve parameter estimates and validate model assumptions. The behavior of parameter estimators in various scenarios and data settings can be investigated through simulation experiments, which provide useful insights into the overall identifiability of the Probabilistic MOGZLL model. Additionally, the accuracy of parameter estimation in real-life and reliability applications can be improved by using robust estimating approaches that are less susceptible to outliers or skewed data distributions.

The Probabilistic MOGZLL model is driven by multiple primary goals in real-life and reliability implementations:

I. By adding new parameters or changing the ones that are already there, the Probabilistic MOGZLL model gets better at describing the different levels of peakedness or flatness that are seen in probability distributions. This increased adaptability makes it possible to match datasets with varying kurtotic properties more precisely, increasing the model's usefulness in a variety of contexts.

II. The model's capacity to add skewness to both symmetrical and asymmetrical distributions is a key driving force. The MOGZLL framework offers tools for efficiently controlling skewness, making it possible to model datasets with intended or intrinsic asymmetry. In domains like finance, economics, and social sciences, where skewed distributions are typical and essential for realistic portrayal, this characteristic is very helpful.

III. The Probabilistic MOGZLL model excels in constructing heavy-tailed densities that maintain computational tractability without excessively long tails. This balance between tail behavior and practicality is crucial for accurately modeling real-life and reliability datasets characterized by heavy-tailed distributions, such as income distributions, extreme event occurrences, and environmental data. By realistically depicting tail behavior, the probabilistic MOGZLL model enhances the reliability and robustness of statistical analyses.

IV. Being better at goodness-of-fit metrics than previous LL extensions is one of the main goals of the probabilistic MOGZLL model. The probabilistic MOGZLL model shows its superior capacity to capture the underlying structure of varied datasets through comparative studies and empirical validation. This capacity not only confirms its effectiveness but also enables practitioners and academics to obtain significant insights and make defensible decisions based on trustworthy statistical studies.

Although the probabilistic MOGZLL model provides an adaptable structure for evaluating survival and dependability information, it is critical to acknowledge its constraints and investigate opportunities for expansion and improvement. Improvements that strengthen the probabilistic MOGZLL model's adaptability, resilience, and suitability for various data scenarios lead to a better comprehension and wider application of the model in real-life and reliability statistical analysis. Its relevance in tackling modern analytical difficulties is ensured by ongoing study into improving its parameters and enhancing its capabilities. Depending on (5), the PDF of the new model is expressed as

$$f_{\underline{\boldsymbol{\Psi}}}(\mathcal{y}) = 2\boldsymbol{a}b\frac{1}{c}\frac{\left(1+\frac{1}{c}\mathcal{y}\right)^{-2a-1}}{\left[1-\overline{b}\left(1+\frac{1}{c}\mathcal{y}\right)^{-2\boldsymbol{a}}\right]^{2}}. \tag{6}$$

Finding the moments of the distribution defined by the provided PDF (mean, variance, skewness, and kurtosis) is the first step in performing moment analysis. This would include utilizing integration techniques to derive formulas for these moments for the PDF $f_{\underline{\boldsymbol{\Psi}}}(\mathcal{y})$ and investigating their dependence on parameters $b, \boldsymbol{a}, c$. Gaining knowledge of these times helps one understand the distribution's structure, central tendency, and spread. Examine the distribution's asymptotic behavior as y approaches 0 and y approaches ∞. Understanding the distribution's tail behavior and convergence characteristics under various parameter configurations may be possible with the use of this approach. Our new probability model's HZRF can be obtained by dividing $f_{\underline{\boldsymbol{\Psi}}}(\mathcal{y})/F_{\underline{\boldsymbol{\Psi}}}(\mathcal{y})$.

We carefully created Figures 1 (right) and 1 (left) in order to examine the adaptability and capabilities of the MOGZLL PDF and the associated hazard rate function (HZRF). These graphic depictions offer important insights into the features and behavior of the probabilistic MOGZLL model at different parameter values. Several plots showing the MOGZLL PDF for carefully selected parameter values are shown in Figure 1 (right). We clarify how variations in the form, position, and size characteristics affect the probability distribution by methodically varying these parameters.

These visualizations allow a thorough analysis of the adaptability of the MOGZLL PDF, demonstrating how well it fits a variety of data patterns and modelling requirements, from skewed to symmetrical distributions.
This viewpoint is enhanced by Figure 2, which displays relevant MOGZLL HZRF graphs. This function provides insights into the dynamic risk associated with the modelled phenomena by showing the rate at which events occur over time. Figure 2 provides a thorough grasp of how the model captures temporal patterns in data by examining how changes in MOGZLL parameters affect the shape and trajectory of the HZRF. The capacity of the probabilistic MOGZLL model to account for a broad variety of hazard rate behaviors, including both monotonic and non-monotonic trends, is demonstrated by these figures. Its adaptability makes it more useful for survival modelling and reliability analysis.

When combined, Figures 1 (right) and 1 (left) offer a potent means of examining the adaptability and usefulness of the probabilistic MOGZLL model in statistical research. These visual aids offer intuitive insights into the MOGZLL PDF and related HZRF across different parameter configurations, which facilitates decision-making and model selection. Furthermore, fresh research (Alqasem et al., 2024) indicates that the probabilistic MOGZLL model may be able to produce novel compound distributions inside the G family. Its usefulness in survival analysis is further supported by studies conducted by Loubna et al. (2024), Teghri et al. (204), and Shehata et al. (2024), as well as by applications in actuarial risk analysis, value-at-risk modelling, and medicine (see Bhatti et al. 2023; Salem et al., 2023; Alizadeh et al., 2023; Alkhayyat et al., 2023; Yousof et al., 2022, 2023a,b; Elbatal et al., 2024; Haskem et al., 2024) further underscore its relevance across diverse fields.

Numerous univariate probabilistic MOGZLL model extensions are presented in the literature, demonstrating the adaptability and versatility of the framework. Innovations on the Weibull LL distribution by Tahir et al. (2015), the one-parameter LL system of densities by Cordeiro et al. (2018), the odd LL and Zografos-Balakrishnan LL distributions by Altun et al. (2018a), and the Rayleigh and exponential derived LL distributions by Elbiely and Yousof (2018) are some of the notable advances. New variants of the Weibull LL distribution have been studied by Nasir et al. (2018) and LL inverse Rayleigh distributions have been studied by Goual and Yousof (2020). When taken as a whole, this research provides a wide range of distributions to the MOGZLL framework, increasing its usefulness in other fields. Furthermore, recent research by Ibrahim and Yousof (2020), Yadav et al. (2020), and Gad et al. (2019) has advanced the theoretical framework and applied applications if the LL distribution family. These studies demonstrate the capacity of probabilistic MOGZLL models to meet challenging modelling problems in several fields and emphasize the models' dynamic evolution and ongoing significance in modern statistical research.

In light of the above descriptions and the traits shown in Figures 1 (left) and 1 (right):
Regarding the PDF for MOGZLL (Figure 1 (right)):

I. According to this description, the probability density function shows one noticeable peak, and its tails skew more towards the right side of the distribution to the extent that they do. This pattern suggests a distribution that is skewed and has a distinct mode.
II. The probability density function in this instance does not have a clear peak, but it does have asymmetric tails that are more prominent on the right side. This points to a distribution with a rightward skew and an undefinable apex.
III. The new density can also be “symmetric density", this shows a skewness-free distribution with a balanced shape.

Regarding the HZRF MOGZLL (Figure 1 (left)):

I. "J-HZRF": This is probably a reference to a hazard zone rate function with a "J"-like form. This pattern indicates a decreasing hazard rate at first, followed by a period of relative stability, and then another significant fall.
II. "Decreasing-constant HZRF": This description points to a hazard zone rate function in which the rate of hazard lowers initially, then steadily rises over time.
III. "Upside down HZRF": This expression describes a hazard zone rate function that seems to be an upside-down "U" since it increases and then drops.
IV. "Decreasing HZRF": This indicates a hazard zone rate function in which there are no appreciable variations, and the hazard rate continuously drops with time.

These thorough explanations provide light on the various patterns and traits that the MOGZLL PDF and HZRF display. They highlight these functions' relevance in many statistical analyses and modelling situations by providing a deeper understanding of how these functions operate under various parameter settings and circumstances.

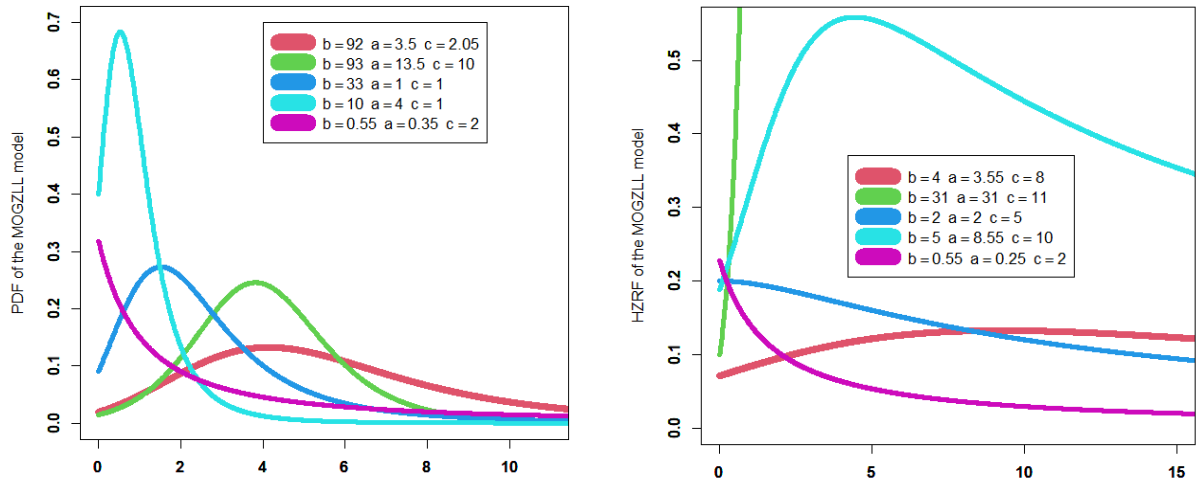

Figure 1: Some PDF plots and HZRF plots under some parameter's values.

The Mean of Order P (MOOP) and PORT-VaR approaches are extensively used in the literature in a variety of sectors, such as risk analysis, insurance, reinsurance, and medicine. In actual applications, these techniques have evolved into essential tools for comprehending and controlling severe occurrences and dangers. Foundational viewpoints on loss modelling and extremal occurrences are presented by Klugman et al. (2012) and Embrechts et al. (2013), respectively. The foundation for useful applications of MOOP in insurance situations is laid by Klugman et al. (2012), who investigate several models for managing and forecasting insurance losses. For the purpose of applying PORT-VaR, Embrechts et al. (2013) explore the theory of extremal events and provide critical insights into the behavior of extreme values. The occurrence and distribution of extraordinary financial events are examined by Jansen and de Vries (1991) and Poon and Rockinger (2003). Their study is especially pertinent to financial contexts for both PORT-VaR and MOOP studies. Poon and Rockinger (2003) examine the statistical characteristics of extreme value distributions in financial markets, while Jansen and de Vries (1991) look into the distribution of extreme financial returns. These studies emphasize how crucial it is to comprehend extreme value behavior in order to quantify and manage risk accurately. The works of Beirlant et al. (2004) and McNeil et al. (2015) provide sophisticated approaches and applications in extreme value theory and risk management. VaR and associated measurements are just a few of the quantitative risk management strategies that are thoroughly covered by McNeil et al. (2015).

The methods for evaluating extreme values and tail risks provided by Beirlant et al. (2004) are crucial for successfully implementing MOOP and PORT-VaR in real-life and reliability scenarios. Their contributions, which incorporate cutting-edge statistical techniques, improve the resilience of risk management strategies. Hosking and Wallis (1987) advance our knowledge of quantile estimation techniques and heavy-tail phenomena. Their work is important for reliability engineering and other domains where extreme values are important for evaluating tail risks. They facilitate the real-life and reliability implementation of PORT-VaR in diverse risk assessment contexts by offering techniques for precisely estimating quantiles in heavy-tailed distributions.

For more recent advancements in statistical modeling and risk analysis see Rasekhi et al. (2022), Hamed et al. (2022), Shrahili et al. (2021), Mohamed et al. (2024), Hashempour et al. (2023), Elbatal et al. (2024), Hamedani et al. (2023). Finally, by introducing an extended Gompertz model, the study of Alizadeh et al. (2024) significantly advances the fields of reliability engineering and risk analysis. The authors offer a thorough methodology for comprehending and handling data on high stresses by combining statistical threshold risk analysis with MOOP assessment. For scholars

and practitioners working with extreme value scenarios, the paper's creative approach and useful applications provide insightful information. On the basis of these results, future studies could increase the validity and range of applications of the model.

The increasing corpus of research on MOOP and PORT-VaR, together with new developments in statistical modelling, highlights how risk analysis techniques are changing. Through the integration of novel models and techniques with traditional approaches, scholars and practitioners can improve their prediction power and make better-informed strategic choices. All of these contributions emphasize how important it is to have strong risk management plans and to keep developing new techniques to deal with complicated and extreme risk situations in a variety of industries.

2. Properties

2.1 Asymptotic and Quantile function (QF)

As $y \to \infty$ the term $\left(1+\frac{1}{c}y\right) \approx \frac{1}{c}y$. Thus, the density function can be approximated by

$$f_{\underline{\Psi}}(y) = 2ab\frac{1}{c}\frac{\left(\frac{1}{c}y\right)^{-2a-1}}{\left[1-\overline{b}\left(\frac{1}{c}y\right)^{-2a}\right]^2}.$$

For large y, $\left(\frac{1}{c}y\right)^{-2a}$ becomes very small, so $1-\overline{b}\left(\frac{1}{c}y\right)^{-2a} \approx 1$. Thus, we have:

$$f_{\underline{\Psi}}(y) = 2ab\left(\frac{1}{c}y\right)^{-2a-1}.$$

This indicates that the density decays polynomial as $y \to \infty$, with a rate proportional to y^{-2a-1}. As $y \to 0$, the term $1+\frac{1}{c}y \approx 1$. Hence $f_{\underline{\Psi}}(y) = \frac{2a}{b}$. The QF of y can be derived by inverting (5), then

$$y_u = \Omega\left[\frac{1}{1-\overline{b}u}(1-u)\right]^{-\frac{1}{a}} - 1, \tag{7}$$

Equation (7) has many applications, and it can be used for simulating the new model.

2.2 Combinations

Let

$$\varpi_{a,c}(y) = 1-\left[\left(\frac{1}{c}y+1\right)^{-1}\right]^{2a},$$

and

$$B_{b,a,c}(y) = 1-\overline{b}-\left[\left(\frac{1}{c}y+1\right)^{-1}\right]^{2a}.$$

Then, by expanding the quantity $\varpi_{a,c}(y)$ we get

$$\varpi_{a,c}(y) = 1+\sum_{v=0}^{+\infty}\binom{2a}{v}(-1)^{v+1}\left[1-\left(\frac{1}{c}y+1\right)^{-2}\right]^{v},$$

which can be repressed as

$$\varpi_{a,c}(y) = \sum_{v=0}^{+\infty}c_v\left[1-\left(\frac{1}{c}y+1\right)^{-2}\right]^{v} \tag{8}$$

where $c_0 = 2$ and

$$c_v = (-1)^{v+1}\binom{2a}{v} | v \geq 1.$$

Analogously, the quantity $B_{b,a,c}(y)$ can be expanded, then we have

$$\boldsymbol{B}_{b,\boldsymbol{a},c}(y) = 1 - \overline{b} - \sum_{\nu=0}^{+\infty} \binom{2\boldsymbol{a}}{\nu} (-1)^{\nu} \left[1 - \left(1 + \frac{1}{c} y\right)^{-2}\right]^{\nu},$$

then

$$\boldsymbol{B}_{b,\boldsymbol{a},c}(y) = \sum_{\nu=0}^{+\infty} d_{\nu} \left[1 - \left(\frac{1}{c} y + 1\right)^{-2}\right]^{\nu}, \tag{9}$$

where $b = d_0$ and

$$d_{\nu} = (1 - b) \binom{2\boldsymbol{a}}{\nu} (-1)^{\nu+1}.$$

Then employing equation (8) and equation (9), the new CDF of the probabilistic MOGZLL model can be simplified as

$$F_{\underline{\boldsymbol{\varphi}}}(y) = \sum_{\nu=0}^{+\infty} \boldsymbol{C}_{\nu} H_{\nu,c}(y), \tag{10}$$

Where function $H_{\nu,c}(y) = W_c^{\nu}(y)$ is the CDF of the well-known exponentiated-LL (exp-LL) model with power positive parameter ν and

$$\boldsymbol{C}_{\nu} = \frac{1}{\boldsymbol{a}_0} \left(c_{\nu} - \frac{1}{d_0} \sum_{i=1}^{\nu} d_i \ \boldsymbol{C}_{\nu-i} \right) | \boldsymbol{C}_0 = \frac{c_0}{d_0} \text{ and } \nu \geq 1.$$

By differentiating (10), we get

$$f_{\underline{\boldsymbol{\varphi}}}(y) = \sum_{\nu=0}^{+\infty} \boldsymbol{C}_{\nu} h_{\nu+1,c}(y), \tag{11}$$

where $h_{\nu+1,c}(y)$ is the exp-LL.

2.3 Moments

The $\boldsymbol{\mathcal{P}}^{th}$ ordinary moment of $\boldsymbol{Y}$ is given by

$$\boldsymbol{U}_{\boldsymbol{\mathcal{P}}}^{'} = E(\boldsymbol{Y}^{\boldsymbol{\mathcal{P}}}) = \int_{-\infty}^{+\infty} y^{\boldsymbol{\mathcal{P}}} f_{\underline{\boldsymbol{\varphi}}}(y) dy.$$

Then, we obtain

$$\boldsymbol{U}_{\boldsymbol{\mathcal{P}}}^{'} = \sum_{\nu=0}^{+\infty} \sum_{\vartheta=0}^{\boldsymbol{\mathcal{P}}} \boldsymbol{C}_{\nu,\vartheta}^{(\boldsymbol{\mathcal{P}},\nu+1)} \boldsymbol{B}(1 + \nu, 1 + \vartheta - \boldsymbol{\mathcal{P}})|_{(1>\boldsymbol{\mathcal{P}})}, \tag{12}$$

where

$$\boldsymbol{C}_{\nu,\vartheta}^{(\boldsymbol{\mathcal{P}},\nu+1)} = \boldsymbol{C}_{\nu}(1 + \nu) c^{\boldsymbol{\mathcal{P}}} (-1)^{\vartheta} \binom{\boldsymbol{\mathcal{P}}}{\vartheta}$$

and

$$\mathbf{B}(1 + \boldsymbol{C}_1, 1 + \boldsymbol{C}_2) = \int_0^1 y^{\boldsymbol{C}_1} (1 - y)^{\boldsymbol{C}_2} dy.$$

Then,

$$E(\boldsymbol{Y}) = \sum_{\nu=0}^{+\infty} \sum_{\vartheta=0}^{1} \boldsymbol{C}_{\nu,\vartheta}^{(1,\nu+1)} \boldsymbol{B}(1 + \nu, \vartheta),$$

$$E(\boldsymbol{Y}^2) = \sum_{\nu=0}^{+\infty} \sum_{\vartheta=0}^{2} \boldsymbol{C}_{\nu,\vartheta}^{(2,\nu+1)} \boldsymbol{B}(1 + \nu, \vartheta - 1),$$

$$E(\boldsymbol{Y}^3) = \sum_{\nu=0}^{+\infty} \sum_{\vartheta=0}^{3} \boldsymbol{C}_{\nu,\vartheta}^{(3,\nu+1)} \boldsymbol{B}(1 + \nu, \vartheta - 2),$$

and

$$E(\boldsymbol{y}^4) = \sum_{\nu=0}^{+\infty}\sum_{\vartheta=0}^{4} \boldsymbol{C}_{\nu,\vartheta}^{(4,\nu+1)}\, \boldsymbol{B}(1+\nu, \vartheta-3),$$

where $E(\boldsymbol{y}) = \boldsymbol{u}_1'$ is the mean of $\boldsymbol{y}$. The $\boldsymbol{\mathcal{P}}^{th}$ incomplete moment, say $I_{\boldsymbol{\mathcal{P}},\boldsymbol{y}}(\mathcal{T})$, of $\boldsymbol{y}$ can be expressed, from (11), as

$$I_{\boldsymbol{\mathcal{P}},\boldsymbol{y}}(\mathcal{T}) = \int_{-\infty}^{\mathcal{T}} f(\boldsymbol{y})\, \boldsymbol{y}^{\boldsymbol{\mathcal{P}}} d\boldsymbol{y} = \sum_{\nu=0}^{+\infty} \boldsymbol{C}_{\nu} \int_{-\infty}^{\mathcal{T}} \boldsymbol{y}^{\boldsymbol{\mathcal{P}}}\, w_{(\nu+1),c}(\boldsymbol{y}) d\boldsymbol{y}$$

then

$$I_{\boldsymbol{\mathcal{P}},\boldsymbol{y}}(\mathcal{T}) = \sum_{\nu=0}^{+\infty}\sum_{\vartheta=0}^{\boldsymbol{\mathcal{P}}} \boldsymbol{C}_{\nu,\vartheta}^{(\boldsymbol{\mathcal{P}},1+\nu)}\, \boldsymbol{B}_{\mathcal{T}}(1+\nu, 1+\vartheta-\boldsymbol{\mathcal{P}})|_{(1>\boldsymbol{\mathcal{P}})},$$

where

$$\boldsymbol{B}_{\cdot}(1+\boldsymbol{C}_1, 1+\boldsymbol{C}_2) = \int_0^{\cdot} \boldsymbol{y}^{\boldsymbol{C}_1}\, (1-\boldsymbol{y})^{\boldsymbol{C}_2} d\boldsymbol{y}.$$

For $\boldsymbol{\mathcal{P}} = 1$, we have

$$I_{1,\boldsymbol{y}}(\mathcal{T}) = \sum_{\nu=0}^{+\infty}\sum_{\vartheta=0}^{1} \boldsymbol{C}_{\nu,\vartheta}^{(\nu+1,1)}\, \boldsymbol{B}_{\mathcal{T}}(\nu+1, \vartheta),$$

which is the first order of the incomplete moment.

2.4 Moment generating functions (GF) and other functions

The moment generating function (MGF) can be derived using (8) as

$$M_{\boldsymbol{y}}(\mathcal{T}) = \sum_{\nu=0}^{+\infty} \boldsymbol{C}_{\nu}\, M_{(1+\nu),c}(\mathcal{T}),$$

where $M_{(1+\nu),c}(\mathcal{T})$ is the MGF of the expLL model, then

$$M_{\boldsymbol{y}}(\mathcal{T}) = \sum_{\nu,\boldsymbol{\mathcal{P}}=0}^{+\infty}\sum_{\vartheta=0}^{\boldsymbol{\mathcal{P}}} \boldsymbol{C}_{\nu,\vartheta,\boldsymbol{\mathcal{P}}}^{(\boldsymbol{\mathcal{P}},\nu+1)}\, \boldsymbol{B}(1+\nu, 1+\vartheta-\boldsymbol{\mathcal{P}})|_{(1>\boldsymbol{\mathcal{P}})},$$

where

$$\boldsymbol{C}_{\nu,\vartheta,\boldsymbol{\mathcal{P}}}^{(\boldsymbol{\mathcal{P}},\nu+1)} = \mathcal{T}^{\boldsymbol{\mathcal{P}}} \boldsymbol{C}_{\nu,\vartheta}^{(\boldsymbol{\mathcal{P}},1+\nu)}/\boldsymbol{\mathcal{P}}!$$

The first $\boldsymbol{\mathcal{P}}$ derivatives of $M_{\boldsymbol{y}}(\mathcal{T})$, with respect to $\mathcal{T}$ at $\mathcal{T} = 0$, yield the first $\boldsymbol{\mathcal{P}}$ moments about the origin, i.e.,

$$\boldsymbol{u}_{\boldsymbol{\mathcal{P}}}' = E(\boldsymbol{y}^{\boldsymbol{\mathcal{P}}}) = \frac{d^{\boldsymbol{\mathcal{P}}}}{d\mathcal{T}^{\boldsymbol{\mathcal{P}}}} M_{\boldsymbol{y}}(\mathcal{T})|\mathcal{T} = 0 \text{ and } \boldsymbol{\mathcal{P}} = 1,2,3,\ldots,$$

The cumulant generating functions (CUGF) say $K_{\boldsymbol{\mathcal{P}}}$, can be obtained from

$$K_{\boldsymbol{\mathcal{P}}} = \frac{d^{\boldsymbol{\mathcal{P}}}}{d\mathcal{T}^{\boldsymbol{\mathcal{P}}}} log\left[\sum_{\nu,\boldsymbol{\mathcal{P}}=0}^{+\infty} \vdots \sum_{\vartheta=0}^{\boldsymbol{\mathcal{P}}} \boldsymbol{C}_{\nu,\vartheta,\boldsymbol{\mathcal{P}}}^{(\boldsymbol{\mathcal{P}},\nu+1)}\, \boldsymbol{B}(\nu+1,1+\vartheta-\boldsymbol{\mathcal{P}})\right]|\mathcal{T} = 0, \text{and } \boldsymbol{\mathcal{P}} = 1,2,\ldots.$$

The 1st CU is the mean ($\nu_1 = \boldsymbol{u}_1'$), the 2nd CU is the variance, and the $\boldsymbol{\mathcal{P}}^{th}$ CU is the same as the third central moment $K_3 = \boldsymbol{u}_3$. But fourth and higher order CUs are not equal to central moments, that being said

$$K_1 = \boldsymbol{u}_1', K_2 = \boldsymbol{u}_2' - \boldsymbol{u}_1'^2 = \boldsymbol{u}_2,$$

and

$$K_3 = \boldsymbol{u}_3' - 3\boldsymbol{u}_2'\boldsymbol{u}_1' + 2\boldsymbol{u}_1'^3 = \boldsymbol{u}_3.$$

Then,

$$K_{\boldsymbol{\mathcal{P}}}|\boldsymbol{\mathcal{P}} \geq 1 = \boldsymbol{u}_{\boldsymbol{\mathcal{P}}}^{'} - \sum_{m=0}^{\boldsymbol{\mathcal{P}}-1} \boldsymbol{u}_{\boldsymbol{\mathcal{P}}-m}^{'} \binom{\boldsymbol{\mathcal{P}}-1}{m-1} \nu_m.$$

2.5 Reversed residual (RVR) life function

The n^{th} moment of the RVR life, say

$$\boldsymbol{r}_{n,\mathcal{T},\boldsymbol{y}}(\mathcal{T}) = I_0^{\mathcal{T}}(y; n) \frac{1}{F_{\underline{\boldsymbol{\varphi}}}(\mathcal{T})},$$

where

$$I_0^{\mathcal{T}}(y|n) = \int_0^{\mathcal{T}} dF(y)\,(\mathcal{T} - y)^n.$$

Then,

$$\boldsymbol{r}_{n,\mathcal{T},\boldsymbol{y}}(\mathcal{T}) = \frac{1}{F(\mathcal{T})} \sum_{\nu=0}^{+\infty} \sum_{\vartheta=0}^{\boldsymbol{\mathcal{P}}} \boldsymbol{C}_{\nu,\vartheta}^{(\nu+1,n)}(\mathcal{T}, \boldsymbol{y}) \boldsymbol{B}_{\mathcal{T}}(\nu + 1, 1 + \vartheta - \boldsymbol{\mathcal{P}})|_{(1>\boldsymbol{\mathcal{P}})},$$

where

$$\boldsymbol{C}_{\nu,\vartheta}^{(\nu+1,n)}(\mathcal{T}, \boldsymbol{y}) = \boldsymbol{C}_{\nu}(\nu + 1) c^{\boldsymbol{\mathcal{P}}} (-1)^{\vartheta} \binom{\boldsymbol{\mathcal{P}}}{\vartheta} \sum_{d=0}^{n} (-1)^d \binom{n}{d} \mathcal{T}^{n-d}.$$

3. Graphical assessment

Graphically and through rigorous statistical analysis involving biases and mean squared errors (MSEs), we conducted extensive simulation experiments to assess the behavior of maximum likelihood estimators (MAX-LEs) for the MOGZLL distribution under varying sample sizes $n|_{(n=50,100,150\ldots,750)}$. This empirical investigation aimed to provide insights into the reliability and precision of parameter estimation in practical scenarios.

The simulation procedure followed a structured approach:

Algorithm I:

We generated N =1000 samples of size n from the MOGZLL distribution, leveraging the formulation detailed in Equation (7).

Algorithm II:

We calculated the Maximum Likelihood Estimators (MAX-LEs) for the parameters Ψ=b,a, and c for each of these N =1000 samples. These estimators are important because they try to find the best values of $\underline{\boldsymbol{\Psi}} = b, \boldsymbol{a}, c$ so that the probabilistic MOGZLL model maximizes the probability of detecting the sampled data.

Algorithm III:

We computed the Standard Errors (SEs) corresponding to the MAX-LEs obtained in Algorithm II in order to assess the accuracy of our calculations. Across the N =1000 samples, these SEs gave us a gauge of the variability or uncertainty in our parameter estimates.

Algorithm IV:

To quantify the accuracy of the MAX-LEs, we computed biases and mean squared errors (MSEs) under the assumption $\underline{\boldsymbol{\Psi}} = b, \boldsymbol{a}, c$ across the range of sample sizes $n|_{(n=50,100,150\ldots,750)}$. Biases, represented as "Bias" indicate the systematic deviation of our estimates from the true parameter values, while MSEs reflect the overall variability and precision of these estimates.

Figure 2 visually presents the outcomes of our simulation study:

i. The left panels of Figure 2 (first row for b, second row for $\boldsymbol{a}$, and third row for c) depict how biases evolve with increasing sample size n. Generally, biases tend towards zero as n increases, indicating improved accuracy in parameter estimation with larger datasets.

ii. First row for b, second row for $\boldsymbol{a}$, and third row for c in the right panels of Figure 2 show the trend of MSEs over various sample sizes n. MSEs drop with increasing n, indicating improved consistency and precision in estimating the three parameters.

These empirical results highlight how well the probabilistic MOGZLL model captures the underlying structure of the data at different sample sizes. The accuracy of the Maximum Likelihood estimation in characterizing the MOGZLL distribution is validated by the convergence of biases towards zero and the lowering of MSEs towards decreasing values. These understandings are essential for academics and practitioners who want to use the probabilistic MOGZLL model in practical statistical studies to ensure trustworthy inference and empirical data-based decision-making.

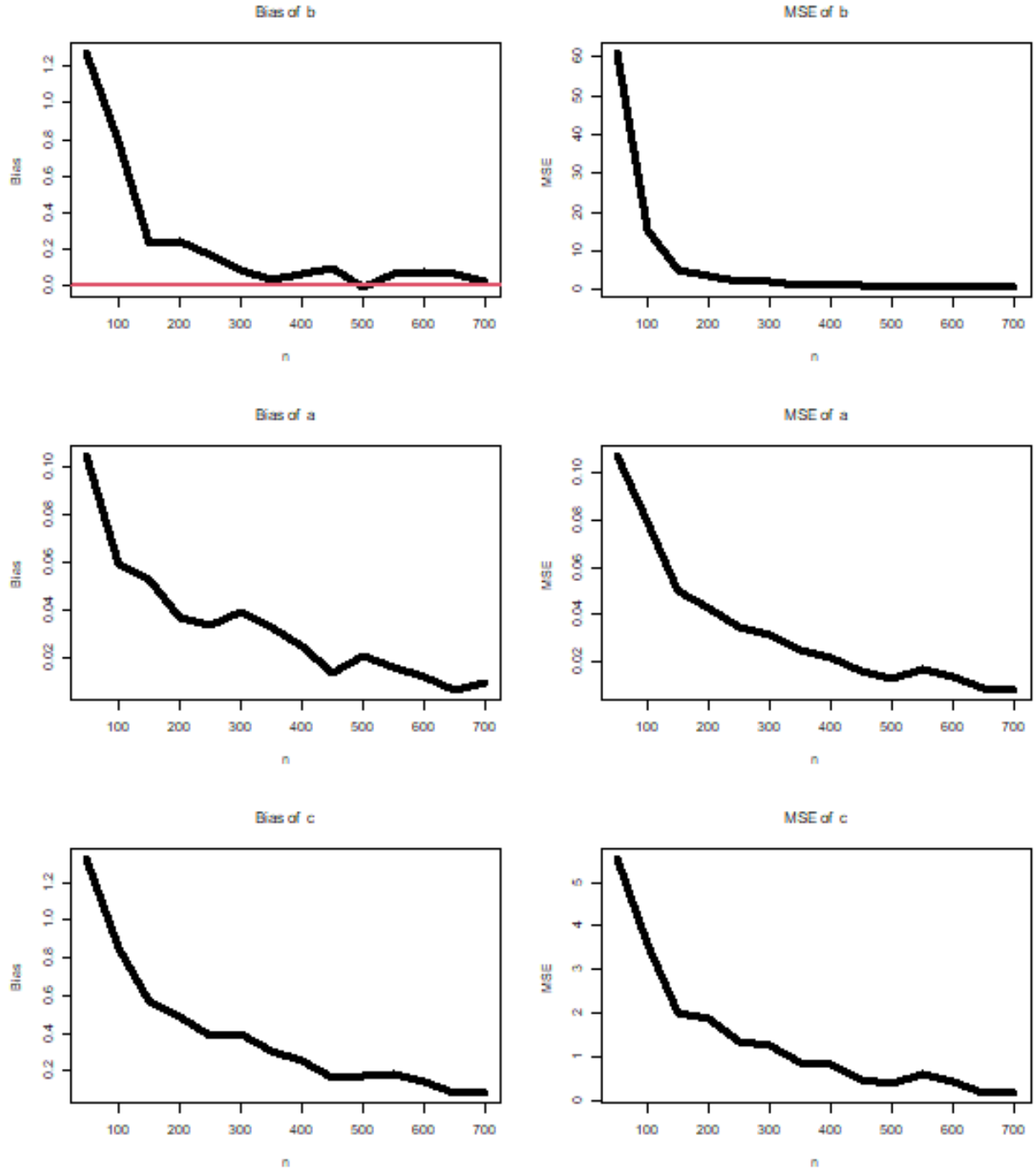

Figure 2: (first row) biases and MSEs for the parameter b,
(second row) biases and MSEs for the parameter a,
(third row) biases and MSEs for the parameter c.

4. Data Analysis

In this section, we want to demonstrate the probabilistic MOGZLL model's adaptability and practical application by analyzing two real datasets. These datasets show how flexible the probabilistic MOGZLL model is in many analytical contexts, in addition to providing real-life and reliability instances. We performed a comparative analysis against other existing models, as shown in Table 1, in order to fully assess its efficacy. The first dataset analyzed, called dataset I, is from a 2004 study by Murthy et al. and is about the failure times of 84 aircraft windscreens.

Our goal in analyzing this dataset is to find out what factors affect the durability and dependability of aircraft windscreens. To ensure operating efficiency, this inquiry is essential for improving aviation safety standards and optimizing maintenance methods. We now focus on the operational dynamics of aircraft maintenance by examining dataset II, which includes the service times of 63 aircraft windscreens from the same study by Murthy et al. By examining service durations, we may spot patterns and trends that help us plan maintenance operations more effectively, reducing downtime and enhancing aircraft performance. Maintaining aircraft reliability and safety requires an understanding of the variables affecting service periods, such as environmental considerations, component wear, and maintenance practices.

The analysis of potential outliers in both datasets was facilitated by box plots (BP), as shown in Figure 3. Notably, Figure 3 showed a consistent distribution of values with no outliers, lending confidence to the dataset's trustworthiness and coherence. To examine the form of the data without imposing parametric assumptions, we used kernel density estimation (N-KDE), as shown in Figure 4. This nonparametric technique visualized the distributional features of the data, providing insights into its underlying shape and dispersion. To delve deeper into the behavior of the datasets over time, we evaluated the Hazard Zone Rate Function (HZRF) with total time in test (TTIT) plots, as shown in Figure 5. The analysis of Figure 5 revealed a "monotonically increasing" trend in the HZRF for both datasets, indicating a consistent pattern of hazard rates across time. To test the dataset’s normality, Quantile-Quantile plots (QQP) were created and analyzed, as shown in Figure 6.

The data points' proximity to the diagonal line in Figure 6 revealed a near approximation to normality, which supported the validity of following statistical studies. Figures 7 and 8 provide a detailed study of the two datasets.

I. The Estimated Probability Density Function (EPDF) visualizes the probability distribution of each dataset, revealing the possibility of certain values happening.
II. The Estimated Cumulative Distribution Function (ECDF) shows the cumulative distribution of data values, offering a full perspective of observation distribution across the dataset.

These analytical tools and visualizations not only enable a complete examination of the dataset’s statistical features, but also serve as a solid platform for deeper insights and informed decision-making in aircraft maintenance management and reliability assessment.

Table 1: Competitive models.

Model	Abbreviation
Lox	Lox
Exponentiated Lox	exp-Lox
Kumaraswamy Lox	KumLox
Macdonald Lox	McLox
Beta Lox	BLox
Gamma Lox	GamLox
Topp-Leone Transmuted Lox	TLTLox
Quasi TLTLox	RTLTLox
Odd LL Lox	OLLLox
Quasi OLLLox	Q-ROLLLox
Quasi Burr-Hatke Lox	Q-BHLox
Special generated mixture Lox	SGMLox
Quasi MOGZLL	Q-MOGZLL
Proportional reversed hazard rate Lox	PRHRLox

Table 1 is an invaluable resource in the field of statistical modelling, giving critical information for model selection and comparison, allowing for more informed decision-making during data analysis and interpretation. We used the "L-BFGS-B" optimization approach to estimate the unknown parameters of each model using maximum likelihood estimation. We used several statistical criteria to evaluate the goodness of fit of these models, including the Akaike Information Criterion (AICR), Bayesian Information Criterion (BICR), Consistent AICR (CAICR), Hannan-Quinn Criterion (HQIC), Anderson-Darling statistic (ϖ^*), and Cramér-von Mises statistic ($\boldsymbol{\varphi}^*$). In general, smaller values of these statistics suggest that the model fits the data better. For computational tasks, we used the "maxLik" and "goftest" subroutines in the R software environment. These tools allowed us to execute the rigorous computations and statistical testing required for model evaluation. Tables 2 and 3 summarize our findings from analyzing the failure time data. Table 2 shows the parameters' Maximum Likelihood Estimates (MAX-LEs) and their related Standard Errors. This table gives information about the precision and reliability of parameter estimates produced from the probabilistic MOGZLL model for the failure time dataset.

Table 3 shows the estimated log-likelihoods and different goodness-of-fit values for the failure time data. These data, including AICR, BICR, CAICR, HQIC, ϖ^*, and $\boldsymbol{\varphi}^*$, were critical in comparing the probabilistic MOGZLL model to other fitted models. The probabilistic MOGZLL model consistently produced the lowest values across these criteria, demonstrating a better fit to the failure times dataset than alternative models. Similarly, for the service times data, we provided our study findings in Tables 4 and 5. Table 4 summarizes the MAX-LEs and SEs derived from fitting the probabilistic MOGZLL model to the service times data, providing a clear picture of parameter estimates and uncertainties.

Table 5 shows the estimated log-likelihoods and goodness-of-fit statistics for the service times dataset. The probabilistic MOGZLL model was shown to have the best match for the service times dataset based on many criteria, including AICR, BICR, CAICR, HQIC, ϖ^*, and $\boldsymbol{\varphi}^*$. A detailed inspection of Tables 4 and 6 reveals that the probabilistic MOGZLL model routinely beats other models in terms of goodness-of-fit statistics for both failure and service time data. Based on these detailed evaluations and statistical comparisons, the probabilistic MOGZLL model emerges as the best option and can be firmly considered the best-fitting model for both datasets. This finding validates the probabilistic MOGZLL model's versatility and robustness in capturing the underlying distributions of complicated real-life and reliability data, bolstering its usefulness in statistical modelling and analysis.

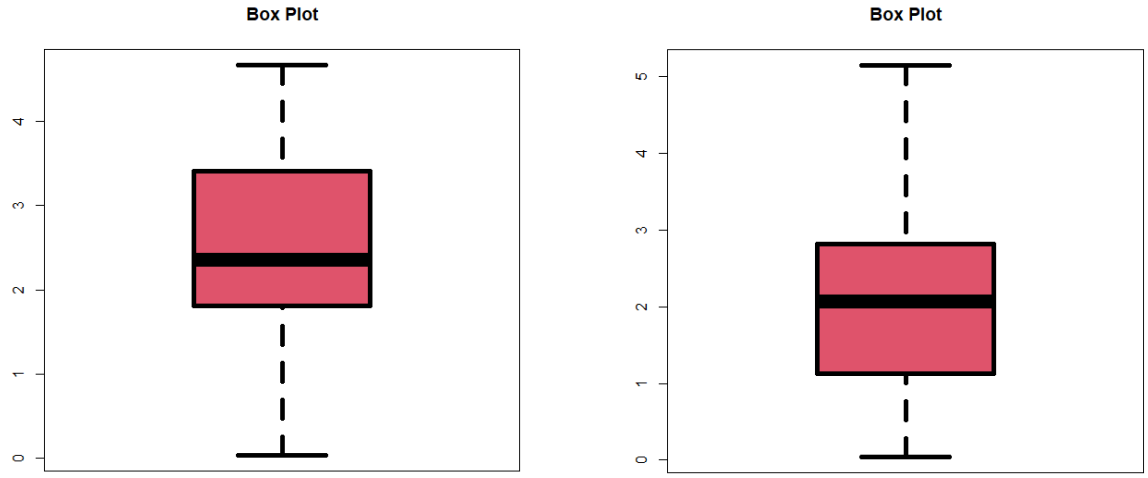

Figure 3: The Box plots for data set **I** (the right panel) and **II** (the left panel).

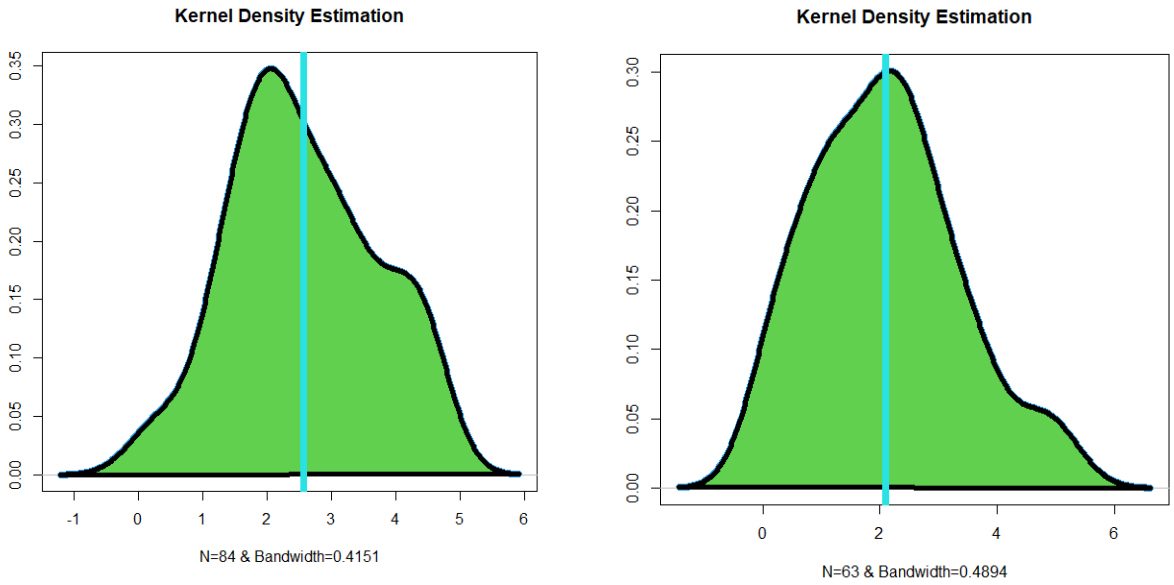

Figure 4: The N-KDEs for data set **I** (the right panel) and **II** (the left panel).

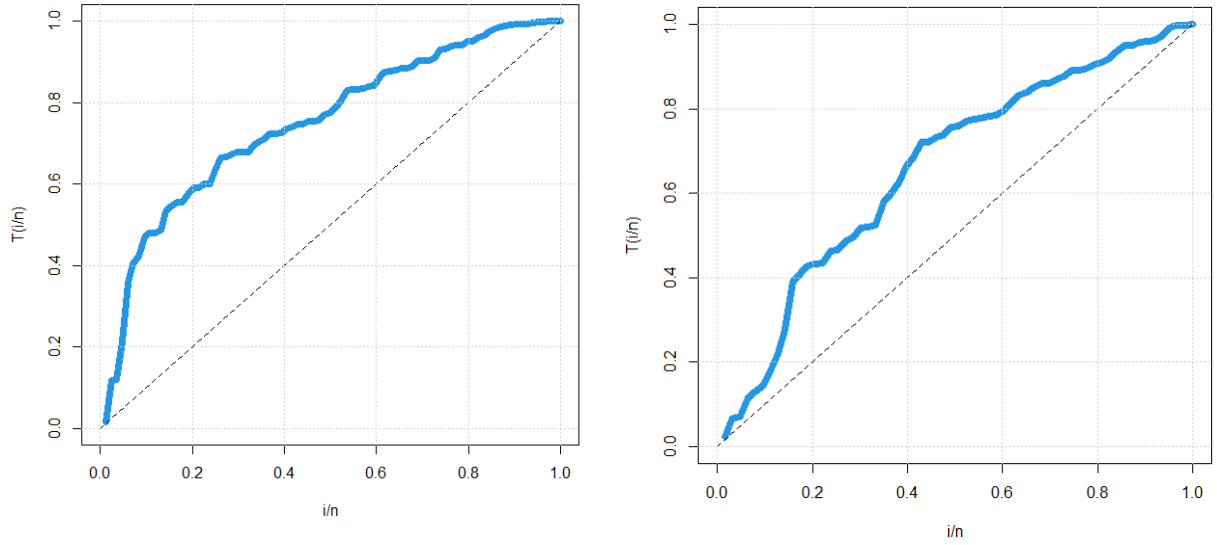

Figure 5: The TTIT plots for data set **I** (the right panel) and **II** (the left panel).

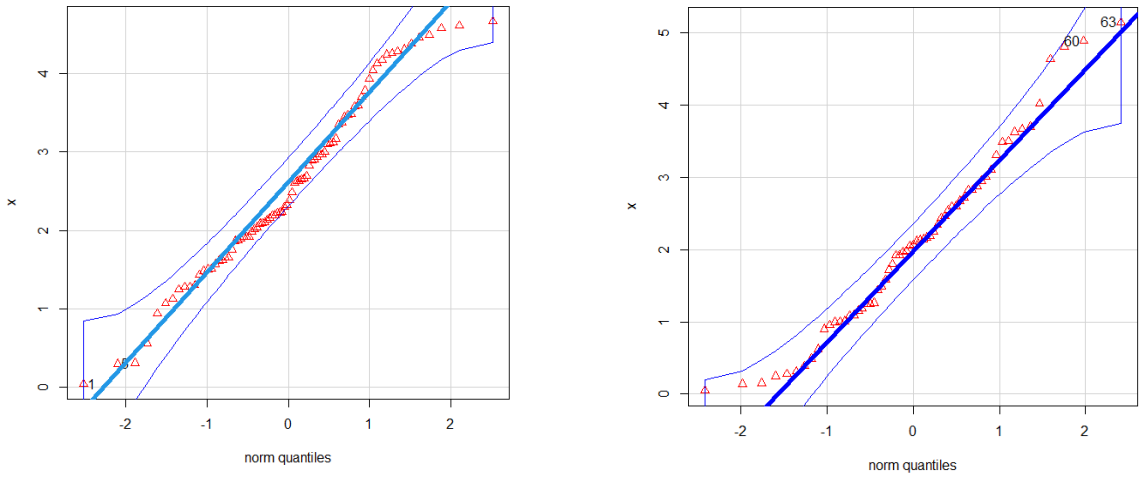

Figure 6: The QQPs for data set **I** (the right panel) and **II** (the left panel).

Table 2: MAX-LEs and SEs for data set **I**.

Model	Estimates				
MOGZLL$(b, \boldsymbol{a}, c)$	**34.598064**	**2.06943×10⁶**	**2.0311×10⁶**		
	(0.008343)	**(0.997033)**	**(0.879842)**		
LMOLox$(b, \boldsymbol{a}, c, a)$	39.655392	27.354543	2.9294416	52.996433	
	2.1551326	(2.006155)	(1.981246)	(1.376435)	
McLox$(b, \boldsymbol{a}, c, \gamma, \beta)$	2.1827451	119.175164	12.413715	19.924343	75.660625
	(0.522113)	(140.29762)	(20.84555)	(38.96045)	(147.2455)
TLTLox$(b, \boldsymbol{a}, c, , \gamma)$	−0.807534	2.47663235	(15608.25)	(38628.34)	
	(0.139642)	(0.5412765)	(1602.3474)	(123.9353)	
KumLox$(b, \boldsymbol{a}, c, , \gamma)$	2.6153021	100.275624	5.2771034	78.677356	
	(0.382233)	(120.48652)	(9.811665)	(186.0037)	
BLox$(b, \boldsymbol{a}, c, , \gamma)$	3.6036504	33.6387054	4.8307063	118.83725	
	(0.618746)	(63.714577)	(9.2382027)	(428.9257)	
PRHRLox$(b, \boldsymbol{a}, c)$	3.7326×10⁶	4.70715×10⁻¹	4.4954×10⁶		
	1.0156×10⁶	(0.0000157)	37.1468434		
RTLTLox$(b, \boldsymbol{a}, c)$	-0.8473253	5.5205762	1.15678547		
	(0.100142)	(1.1847921)	(0.095846)		
SGMLox$(b, \boldsymbol{a}, c)$	-1.0445×10⁻¹	9.8352×10⁶	1.1834×10⁷		
	(0.124235)	(4843.3444)	(501.3047)		
Q-MOGZLL$(b, \boldsymbol{a}, c)$	3.0011673	0.6675324	0.7753213		
	(0.2752135)	(0.008766)	(0.1165155)		
OLLLox$(b, \boldsymbol{a}, c)$	2.3263667	(7.1734×10⁵)	2.3455×10⁶)		
	(2.1383×10⁻¹)	(1.1945×10⁴)	(2.616×10¹)		
GamLox$(b, \boldsymbol{a}, c)$	3.58760444	52004.496	37029.6626		
	(0.5133655)	(7955.0053)	(81.164429)		
exp-LL$(b, \boldsymbol{a}, c)$	3.6261055	20074.5145	26257.684		
	(0.623665)	(2041.8355)	(99.741795)		
Q-ROLLLox$(\boldsymbol{a}, c)$	3.8905647	0.57316564			
	(0.3652464)	(0.0194642)			
Q-BHLox$(\boldsymbol{a}, c)$	10801754.43	51367189			
	(983309.45)	(232312.431)			

Lox$(\boldsymbol{a}, c)$	51425.35604	131789.859
	(5933.4952)	(296.11959)
LL(c)	2.28437536	
	(0.3648298)	

Table 3: GOF statistics for data set **I**.

Model	$-\ell(\underline{\widehat{\boldsymbol{\Psi}}})$	AIFC	CAIFC	BIFC	HQIFC	ϖ^*	$\boldsymbol{\varphi}^*$
MOGZLL	**128.09091**	**261.21353**	**262.10544**	**269.70831**	**265.13001**	**0.50111**	**0.065993**
LMOLox	128.34034	264.68015	265.18651	274.40319	268.58944	0.50915	0.064342
McLox	129.80221	269.60432	270.36443	281.81743	274.51749	0.66713	0.085721
Q-MOGZLL	132.19945	270.39845	270.69834	277.69163	273.33071	0.75989	0.077419
OLLLox	134.42342	274.84733	275.14775	282.13924	277.77892	0.94089	0.100918
TLTLox	135.57052	279.14045	279.64690	288.86365	283.04858	1.12586	0.127798
GamLox	138.40445	282.80825	283.10464	290.13697	285.75537	1.36618	0.161865
BLox	138.71764	285.43545	285.93530	295.20528	289.36535	1.40881	0.168495
exp-LL	141.39934	288.79966	289.09543	296.12758	291.74068	1.74358	0.219865
Q-ROLLLox	142.84543	289.69085	289.83854	294.55231	291.64445	1.95674	0.255785
SGMLox	143.08754	292.17493	292.47442	299.46799	295.10653	1.34657	0.157652
RTLTLox	153.98494	313.96173	314.26143	321.25453	316.89337	3.75264	0.55955
PRHRLox	162.87752	331.75452	332.05445	339.04629	334.68588	1.36747	0.160854
Lox	164.98863	333.97654	334.12346	338.86125	335.94144	1.39478	0.166543
Q-BHLox	168.60452	341.20913	341.35684	346.06912	343.16264	1.64714	0.206789
LL	190.91382	383.82753	383.87635	386.25838	384.80347	2.94589	0.417582

Table 4: MAX-LEs and SEs for data set **II**.

Model	Estimates			
MOGZLL$(b, \boldsymbol{a}, c)$	**9. 0980213**	**9.15329×10^{6}**	**7.8183×10^{6}**	
	(1.901904)	**(4.8911092)**	**(28.544322)**	
LMOLox$(b, \boldsymbol{a}, c, \gamma)$	10.613244	2.6823536	12.645425	26.289265
	(6.139236)	(4.484249)	(21.14253)	(53.72264)
KumLox$(b, \boldsymbol{a}, c, \gamma)$	1.6691425	60.567933	2.556494	65.064325
	(0.257044)	(86.01329)	(4.758945)	(177.5934)
BLox$(b, \boldsymbol{a}, c, \gamma)$	1.9218246	31.259449	4.9684365	169.57186
	(0.3184755)	(316.84146)	(50.528296)	(339.2068)
TLTLox$(b, \boldsymbol{a}, c, \gamma)$	(-0.60756)	1.78578464	2123.39164	4822.7875
	(0.2137454)	(0.415255)	(163.96153)	(200.08742)
PRHRLox$(b, \boldsymbol{a}, c)$	1.59343×10^{6}	3.9377×10^{-1}	1.3014×10^{6}	
	2.01553×10^{3}	0.0042×10^{-1}	0.9543×10^{6}	
RTLTLox$(b, \boldsymbol{a}, c)$	-0.671457	2.74496554	1.0123779	
	(0.1874645)	(0.669646)	(0.1140464)	
SGMLox$(b, \boldsymbol{a}, c)$	-1.0445×10^{-1}	6.4536×10^{6}	6.3335×10^{6}	
	(4.135×10^{-10})	(3.2145×10^{6})	(3.8573155)	
Q-MOGZLL$(b, \boldsymbol{a}, c)$	1.92707143	1.34982495	0.4366035	
	(0.2109635)	(12.647321)	(4.090553)	
OLLLox$(b, \boldsymbol{a}, c)$	1.6641984	6.34315×10^{5}	2.0167×10^{6}	
	(1.7925×10^{-1})	(1.683210^{4})	7.2245×10^{6}	
GamLox$(b, \boldsymbol{a}, c)$	1.90731243	35842.4236	39197.535	
	(0.3213355)	(6945.034)	(151.6534)	
exp-LL$(b, \boldsymbol{a}, c)$	1.9145448	22971.1566	32880.935	
	(0.348198)	(3209.5374)	(162.2336)	
Q-ROLLLox$(\boldsymbol{a}, c)$	2.3723339	0.6910946		
	(0.2682451)	(0.04488294)		

Q-BHLox$(\boldsymbol{a}, c)$	140555219	53203423.46
	(422.00537)	(28.5232345)
Lox$(\boldsymbol{a}, c)$	99269.7847	207019.3653
	(11863.535)	(301.236613)
Lox(c)	1.6750435	
	(0.319985)	

Table 5: GOF statistics for data set **II**.

Model	$-\ell(\underline{\hat{\boldsymbol{\Psi}}})$	AIFC	CAIFC	BIFC	HQIFC	ϖ^*	$\boldsymbol{\varphi}^*$
MOGZLL	**98.218432**	**203.33322**	**203.56092**	**209.72544**	**205.86557**	**0.271794**	**0.042487**
LMOLox	98.918186	205.83622	206.52645	214.40856	209.20852	0.293643	0.046935
KumLox	100.86771	209.73525	210.42463	218.30743	213.10623	0.739643	0.121944
Q-MOGZLL	101.83477	209.66964	210.07674	216.09934	212.12984	0.883921	0.145930
TLTLox	102.44994	212.89980	213.58924	221.47524	216.27219	0.943432	0.155445
GamLox	102.83314	211.66645	212.07355	218.09637	214.19251	1.112643	0.183606
SGMLox	102.89444	211.78853	212.19478	218.21793	214.31645	1.113549	0.183944
BLox	102.96145	213.92250	214.61335	222.49424	217.29333	1.133790	0.187199
exp-LL	103.54906	213.09943	213.50322	219.52831	215.62862	1.233532	0.203777
OLLLox	104.90439	215.80854	216.21530	222.23794	218.33622	0.942965	0.154545
PRHRLox	109.29845	224.59741	225.00443	231.02616	227.12692	1.126321	0.186138
Lox	109.29833	222.59782	222.79739	226.88293	224.28326	1.126032	0.186169
Q-ROLLLox	110.72834	225.45788	225.65725	229.74296	227.14346	2.347434	0.390881
RTLTLox	112.18546	230.37191	230.777437	236.80326	232.89969	2.687986	0.453172
Q-BHLox	112.60054	229.20110	229.401173	233.48735	230.88649	1.398476	0.231683
LL	127.32434	256.64875	256.71432	258.79189	257.49156	2.516501	0.424356

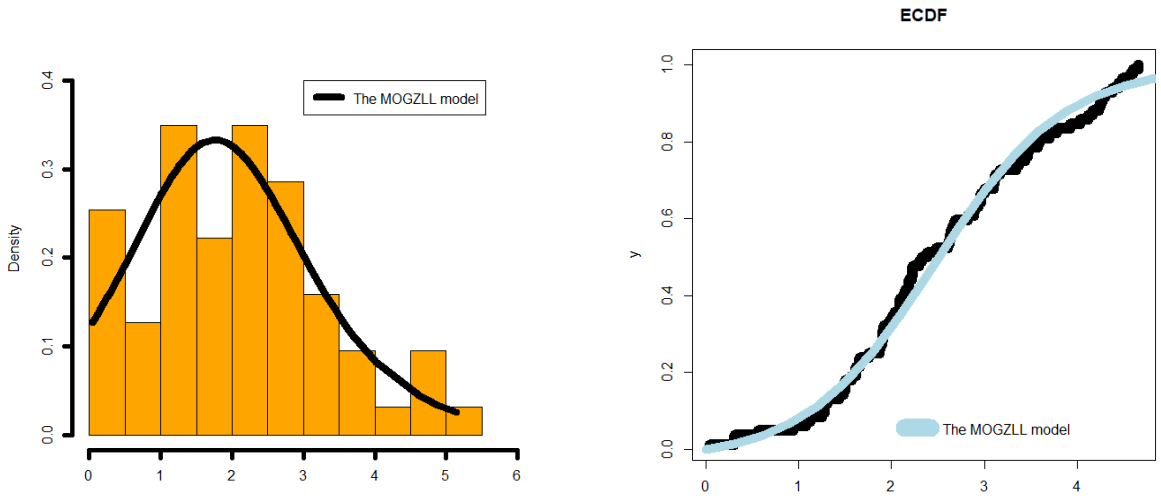

Figure 10: the EPDF and ECDF for data set **I**.

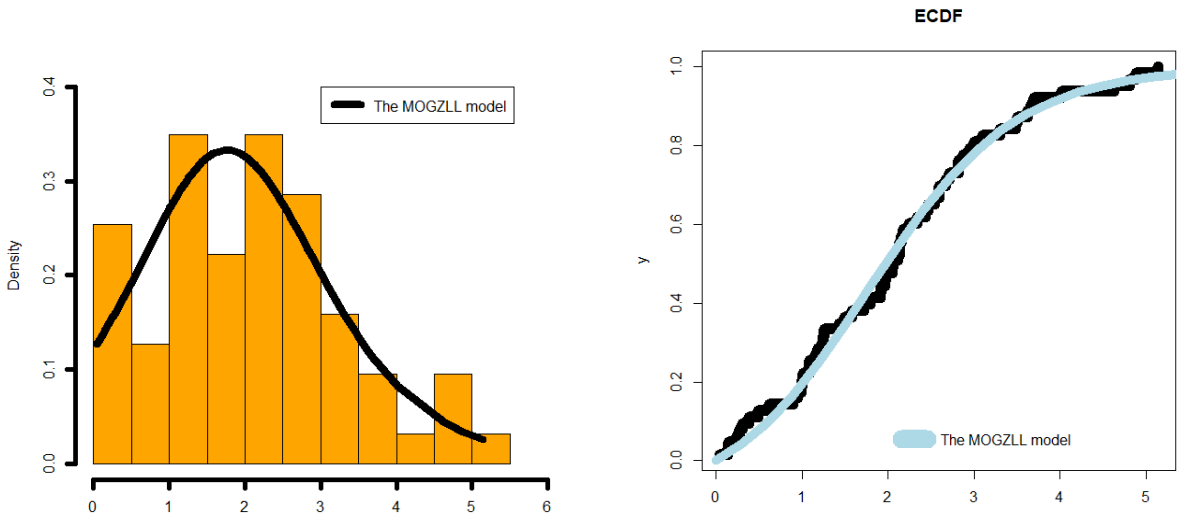

Figure 11: the EPDF and ECDF for data set **II**.

5. PORT-VaR analysis under the Norwegian fire financial claims

The initial dataset used in this study consists of 9181 fire insurance claims with monetary values in thousands of Norwegian kroner (TNOK). These claims, obtained from a Norwegian insurance firm, provide insight into the financial implications of fire-related damages. A significant aspect of this dataset is the use of a deductible threshold of 500 TNOK. This means that only claims over this value were included in the dataset, thereby screening out lesser claims and focusing the research on larger losses. This strategy not only helps to focus on the most important claims, but it also aligns the dataset with specific insurance policy features and financial criteria relevant to the study. The dataset is available through the R package ReIn, which is a specialized tool for working with insurance data. The ReIn package is a great resource for researchers and analysts undertaking detailed investigations on insurance loss modelling. It improves access to precise data and analytical capabilities, increasing the breadth and precision of study in this area.

According to Alizadeh et al. (2024), the PORT-VaR technique is intended to focus on the tail of the loss distribution, focussing on extreme values that surpass a predetermined threshold. For fire insurance claims, this means that PORT-VaR aids in comprehending the financial impact of very big claims, which are frequently the most crucial to insurers. Given the dataset's deductible barrier of 500 TNOK, PORT-VaR is best suited to analyzing claims that are significantly higher than this threshold, capturing the most severe and possibly financially devastating losses. PORT-VaR allows insurers to estimate the potential risk associated with extreme losses above a given threshold. This calculation is critical for successful risk management and establishing sufficient financial reserves to handle future significant claims.

Accurate evaluation of extreme risk aids insurance firms' strategic financial planning, ensuring that they have enough capital to address rare but significant disasters. PORT-VaR is a revised method for modelling the risk associated with the higher tail of the loss distribution. This enables more precise forecasts of the frequency and severity of catastrophic losses, which is critical when pricing insurance policies and anticipating future financial exposures. By analysing peaks that exceed a random threshold, insurers may better estimate the likelihood and extent of major fire claims, resulting in more robust and accurate loss forecasts. Many regulatory systems require insurers to assess and report their exposure to severe risks.

The PORT-VaR contributes to achieving these regulatory criteria by establishing a comprehensive method for assessing the possible impact of extreme fire claims. This research promotes transparent reporting methods by providing a clear and quantitative measure of severe risk that can be shared with stakeholders, regulators, and policyholders. Table 6 presents an in-depth PORT-VaR analysis of Norwegian fire financial claims, organised by confidence level (CL). Each row in the table corresponds to a given confidence level and describes the number of extreme loss events (PORTs) found. It also contains statistical indicators like the minimum (Min.L), first quartile (1^{st} Qu.), median (Median), anticipated value of extreme financial losses (EVL), third quartile (3^{rd} Qu.), and maximum (Max.L) values for these events. The table demonstrates that as confidence levels grow, so does the number of extreme loss events (PORT), indicating a reduced threshold for detecting substantial deviations or outliers in indemnity losses. The statistical measurements provide information on the distribution and severity of these high loss episodes across distinct CLs. For example, maximum values (Max.L) indicate the most severe losses identified at each confidence level. This study is critical for a full risk assessment, as it allows insurance firms to analyze the impact of high loss events at different levels of confidence. This information is critical for optimizing risk management strategies and implementing effective risk mitigation actions. Overall, Table 6 is an invaluable resource for risk analysts and insurance professionals, assisting them in making educated decisions and managing risks associated with Norwegian fire financial claims. The extensive statistical information improves comprehension of risk exposures at various confidence levels, hence facilitating comprehensive risk assessment and mitigation actions in the insurance sector.

Figure 9 also depicts the number of extreme loss events (PORT) for each confidence level (CLs ranging from 20% to 99%), while Figure 10 shows visual graphs of the number of PORT-VaR against the respective confidence levels. Figure 12 shows all of the histograms for the PORT VaR results. Figure 13 depicts the density of peaks.

Table 6: PORT-VaR analysis for the Norwegian fire financial claims.

CLs	VaR	N. of PORT	Min.L	1^{st} Qu.	Median	EVL	3^{rd} Qu.	Max.L
%50	2299	14	2320	3559	3966	4044	4340	6283
%55	2267.8	15	2278	3483	3932	3926	4325	6283
%60	2007.6	17	2023	3215	3747	3717	4295	6283
%65	1817.3	18	1946	2544	3724	3618	4259	6283
%70	1541	19	1712	2299	3702	3518	4222	6283
%75	1299.5	21	1320	2266	3511	3318	4150	6283
%80	1203.2	22	1238	2084	3483	3224	4113	6283
%85	1065.05	23	1180	1984	3455	3135	4076	6283
%90	857.9	25	956	1712	3215	2965	4001	6283
%95	601.7	26	629	1570	2768	2875	3984	6283

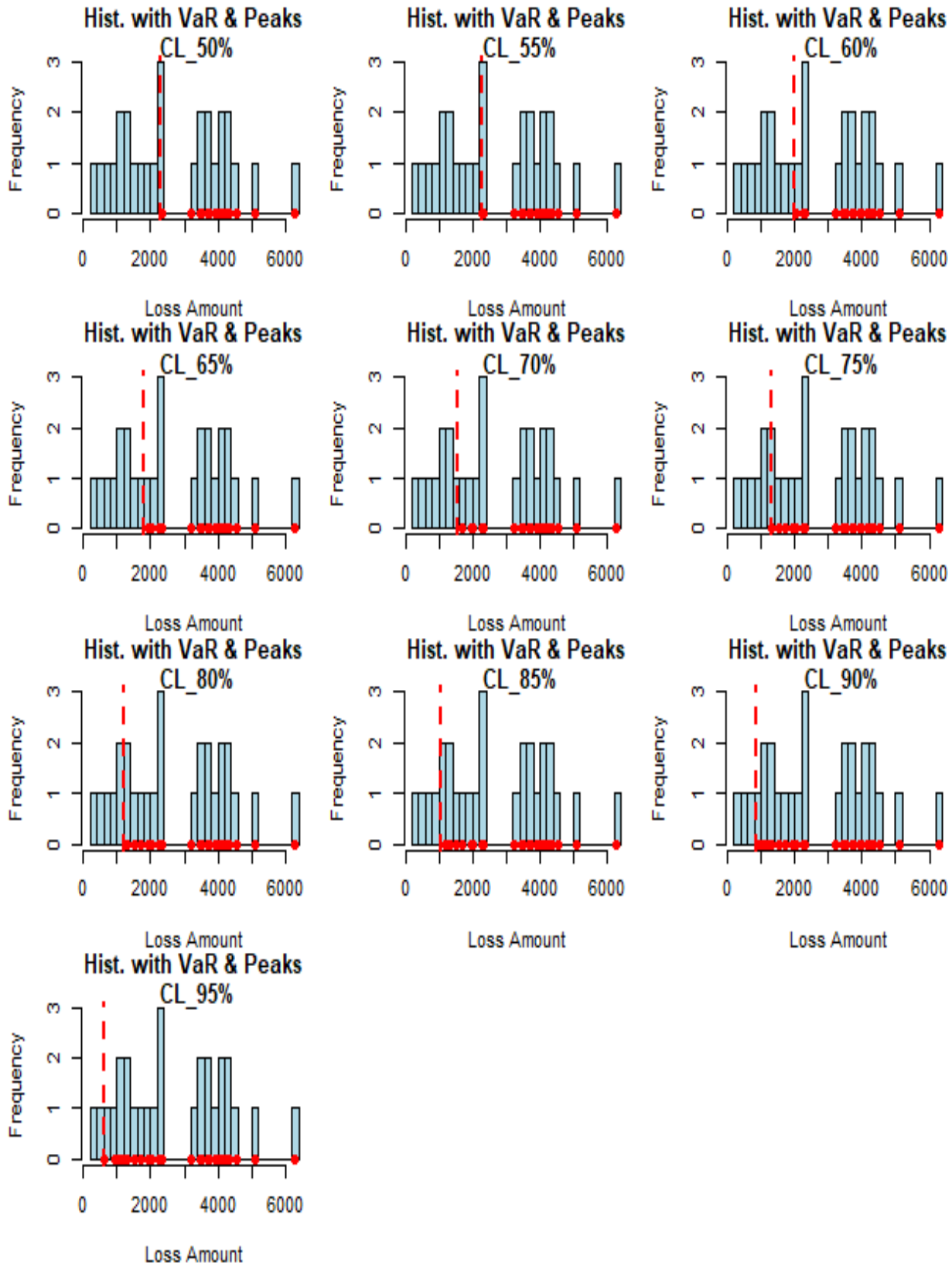

Figure 12: Histograms for the PORT VaR results.

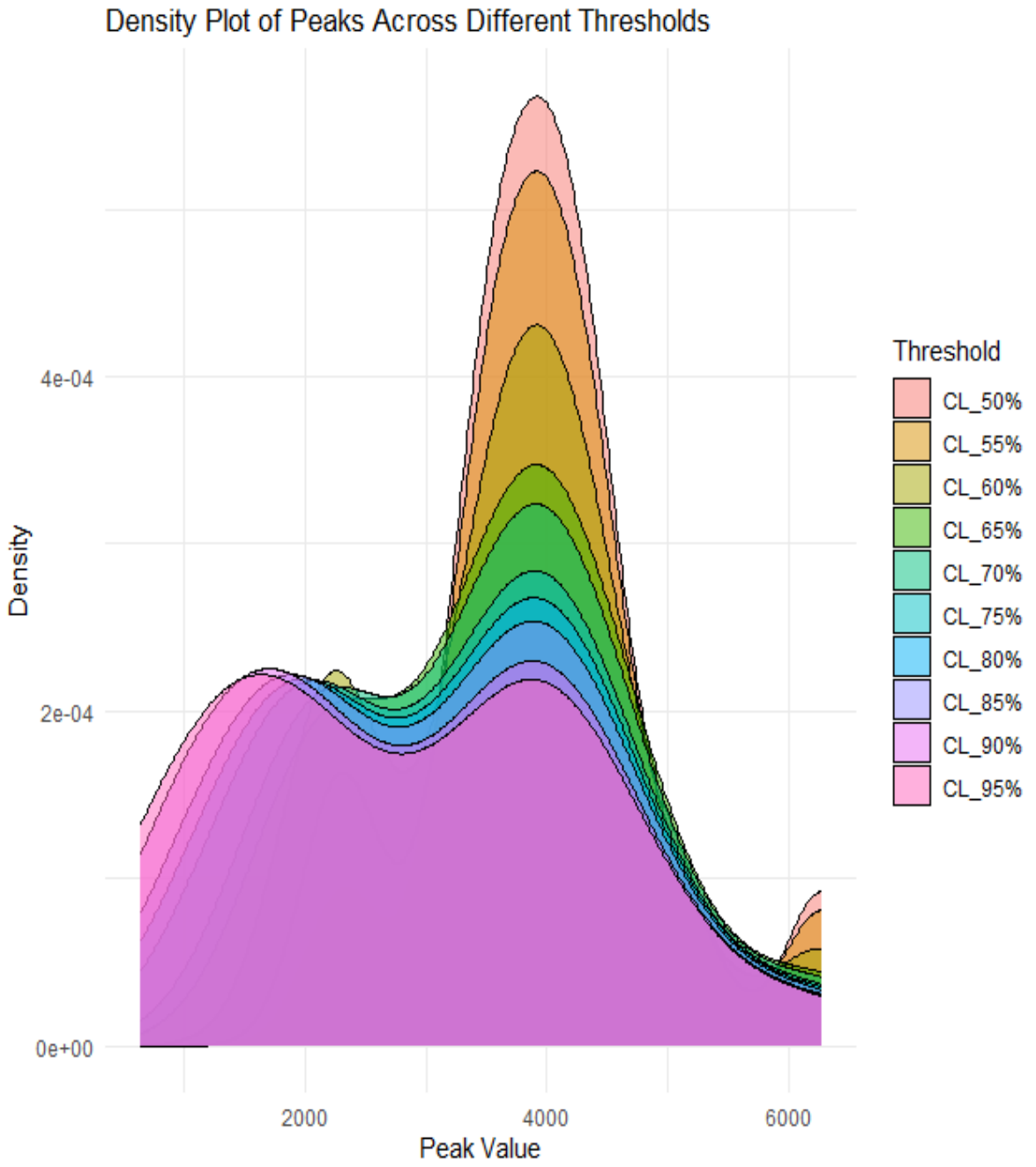

Figure 13: Density of peaks.

Based on the PORT-VaR analysis provided in Table 6, we can draw several conclusions and make financial recommendations regarding Norwegian fire financial claims. The table presents VaR at various CLs along with statistics on the peaks above each VaR threshold. Here's a detailed breakdown:

I. As the CL increases, the VaR decreases. This indicates that higher confidence levels are associated with lower thresholds for identifying extreme loss events.

II. The number of peaks above the VaR threshold increases with higher confidence levels, which suggests that more extreme loss events are identified as the threshold for "extreme" losses is lowered.

III. The minimum peak value increases as the confidence level increases, showing that extreme losses are getting larger.
IV. The 1st quartile value of peaks shows an upward trend with higher confidence levels, indicating that a higher proportion of extreme losses are larger.
V. The median value of peaks increases with higher confidence levels, reflecting that the typical size of extreme losses is higher when considering more extreme confidence levels
VI. The EVL also increases with higher confidence levels, suggesting that the expected size of extreme losses grows as the threshold becomes more conservative.

On the other hand, it is worth mentioning the following financial recommendations can be spotted:

I. Insurers should tailor their risk management strategies based on their risk appetite. For example, if the focus is on more conservative risk management, thresholds corresponding to higher confidence levels (e.g., 90% or 95%) should be considered. Consider the increasing size of extreme losses as confidence levels rise. This indicates that as the threshold gets more cautious, both the frequency and magnitude of extreme losses rise. Financial models should take into consideration these bigger potential losses.
II. II. Increased confidence levels lead to higher expected values of extreme losses (EVL) and more peaks above VaR. Insurers should set aside more cash to cover any losses linked with increased confidence levels. Implement stress tests that take into account extreme loss scenarios discovered with greater confidence levels to guarantee that the insurer can sustain significant financial shocks.
III. III. Premium pricing should consider the possibility of extreme loss events. Insurers may need to raise premiums to cover greater-risk losses recognized at higher confidence levels.
IV. IV. Ensure reserves are sufficient to cover excessive losses. The data implies that if the thresholds for extreme losses become more conservative, the required reserves would rise.
V. Ensure risk management techniques meet regulatory criteria for capital reserves and risk exposure. Regulators may mandate insurers to cover losses at specific confidence levels, which should be factored into the VaR analysis.
VI. Diversifying the portfolio can help lessen the impact of excessive losses. Extreme loss events detected with higher confidence levels may suggest potential risk concentrations that can be handled by diversification techniques.

6. Conclusions

The Marshall-Olkin generated log-logistic (MOGZLL) distribution is a novel three-parameter probability distribution for lifetime data that is introduced and thoroughly investigated in this study. This newly established distribution is thoroughly characterized, demonstrating its versatility and application to a wide range of datasets. The density function of the MOGZLL distribution is intended to demonstrate both right-skewness and symmetry, making it appropriate for modelling datasets with varied asymmetries. Its skewness coefficient supports a wide range of asymmetry representations, including negative and positive skewness values. This flexibility is critical for accurately representing the form and spread of real-life and reliability data distributions. Furthermore, the hazard rate function for the MOGZLL distribution exhibits a variety of characteristics, including monotonic increase, increasing-constant, constant, upside-down, and monotonic drop. This unpredictability allows the MOGZLL distribution to effectively reflect varied patterns of risk or failure rates across time, increasing its usefulness in reliability analysis and survival modelling. The MOGZLL distribution's parameters are estimated using the maximum likelihood approach, which ensures robust and efficient estimation from observed data. A comprehensive simulation analysis is carried out to evaluate the finite-sample behavior of maximum likelihood estimators, including biases and mean squared errors across different sample sizes and circumstances. This rigorous evaluation reveals insights into the estimators' accuracy and dependability under various settings, demonstrating their practical utility in statistical investigations.

Overall, the study highlights the MOGZLL distribution as a powerful statistical modelling tool, providing the flexibility, resilience, and accuracy required for analyzing lifetime data in a variety of sectors including finance, engineering, epidemiology, and more. Through extensive characterization, methodological extensions, and rigorous validation, the MOGZLL distribution emerges as a valuable addition to the repertory of probabilistic models for complex data analysis and inference. The research paper's findings on the MOGZLL distribution shed light on its practical utility and robustness in statistical models.

Here's a debate that builds on these findings:

I. The MOGZLL distribution's ability to combine right-skewness and symmetry in its density function makes it very adaptable to diverse datasets. This adaptability is critical in real applications where data can have varied degrees of asymmetry. Because the skewness coefficient can take both positive and negative values, the MOGZLL distribution can accurately describe the many distributional forms observed in real-life and reliability situations. This feature makes it more suitable for modelling data in a variety of domains, including finance and healthcare.

II. The MOGZLL distribution's hazard rate function (HZRF) has various profiles, allowing it to capture complicated temporal trends in data. Whether the hazard rate increases monotonically, remains constant, or has an upside-down U-shape, the MOGZLL distribution can handle these behaviors. This adaptability is especially useful in survival analysis and reliability engineering, where recognizing the changing nature of risk over time is crucial for decision-making and resource allocation.

III. The use of maximum likelihood estimation (MLE) for parameter estimation ensures reliable and efficient inference from observed data. The extensive simulation research used to assess MLE performance under numerous circumstances gives empirical evidence of the distribution's reliability. Assessing biases and mean squared errors across different sample sizes allows us to assess the accuracy of parameter estimations and gain confidence in the MOGZLL distribution's practical applicability.

IV. The practical ramifications of using the MOGZLL distribution are enormous. The probabilistic MOGZLL model allows for more accurate modelling of complex datasets seen in real-life and reliability contexts because it combines flexibility, robustness, and interpretability. This not only improves the precision of statistical analysis, but it also allows for more informed decision-making in a variety of sectors, including industrial engineering and public health.

V. According to Hashem et al. (2024), the novel probabilistic MOGZLL model enables the presentation of fresh Bayesian results in inference using accelerated models.

To summarize, the MOGZLL distribution provides a substantial improvement in probabilistic modelling, solving important issues in data analysis through its diverse properties and methodological characteristics. The results show that it is effective at capturing the intricacies of real-life data distributions and has the potential to promote research and application in a variety of scientific and industrial fields. Continued research and implementation of the MOGZLL distribution are expected to improve its capabilities and broaden its utility in future statistical techniques. For more useful distributions for the financial applications and risk analysis see Nofal et al. (2016), Alizadeh et al. (2018a,b), El-Morshedy et al. (2021), Korkmaz et al. (2017, 2022), Yousof et al. (2018), Elgohari et al. (2021), Mansour et al. (2020a-e), Rasekhi et al. (2020), Hashem et al. (2024), Elsayed and Yousof (2021, 2020, and 2019a, b), Elbiely and Yousof (2018) and Elbiely and Yousof (2019a,b), Korkmaz et al. (2019), Teghri et al. (2024), Elgohari and Yousof (2020a,b,c), Loubna et al. (2024), and Yousof et al. (2024 and 2016).

References

1. Aarset, M. V. (1987). How to identify a bathtub hazard rate. IEEE Transactions on Reliability, 36(1), 106-108.
2. Alqasem, O. A., Alsheikh, S. M. A., Alsuhabi, H., Aldallal, R., Alsolmi, M. M., Yousof, H. M., ... & Hashem, A. F. (2024). A novel compound G family with properties, copulas, modelling the asymmetric and positive-skewed engineering and medical data. Alexandria Engineering Journal, 98, 80-96.
3. Alizadeh, M., Lak, F., Rasekhi, M., Ramires, T. G., Yousof, H. M., & Altun, E. (2018a). The odd log-logistic Topp–Leone G family of distributions: heteroscedastic regression models and applications. Computational Statistics, 33, 1217-1244.
4. Alizadeh, M., Yousof, H. M., Rasekhi, M., & Altun, E. (2018b). The odd log-logistic Poisson-G Family of distributions. Journal of Mathematical Extension, 12(1), 81-104.
5. Alkhayyat, S. L., Mohamed, H. S., Butt, N. S., Yousof, H. M., & Ali, E. I. (2023). Modeling the Asymmetric Reinsurance Revenues Data using the Partially Autoregressive Time Series Model: Statistical Forecasting and Residuals Analysis. Pakistan Journal of Statistics and Operation Research, 425-446.
6. Atkinson, A. B. and Harrison, A. J. (1978). Distribution of Personal Wealth in Britain (Cambridge University Press, Cambridge).
7. Alizadeh, M., Afshari, M., Contreras-Reyes, J. E., Mazarei, D. and H. M. Yousof, "The Extended Gompertz Model: Applications, Mean of Order P Assessment and Statistical Threshold Risk Analysis Based on Extreme Stresses Data," in IEEE Transactions on Reliability, doi: 10.1109/TR.2024.3425278.
8. Alizadeh, M., Afshari, M., Ranjbar, V., Merovci, F., & Yousof, H. M. (2023). A novel XGamma extension: applications and actuarial risk analysis under the reinsurance data. São Paulo Journal of Mathematical Sciences, 1-31.

9. Altun, E., Yousof, H. M. and Hamedani, G. G. (2018a). A new log-location regression model with influence diagnostics and residual analysis. Facta Universitatis, Series: Mathematics and Informatics, 33(3), 417-449.
10. Altun, E., Yousof, H. M., Chakraborty, S. and Handique, L. (2018b). Zografos-Balakrishnan Burr XII distribution: regression modeling and applications. International Journal of Mathematics and Statistics, 19(3), 46-70.
11. Aryal, G. R., Ortega, E. M., Hamedani, G. G. and Yousof, H. M. (2017). The Topp Leone Generated Weibull distribution: regression model, characterizations and applications, International Journal of Statistics and Probability, 6, 126-141.
12. Atkinson, A.B. and Harrison, A.J. (1978). Distribution of Personal Wealth in Britain (Cambridge University Press, Cambridge).
13. Balkema, A.A. and de Hann, L. Residual life at great age, Annals of Probability 2, 972-804, 1974.
14. Beirlant, J., Goegebeur, Y., Segers, J., & Teugels, J. (2004). Statistics of Extremes: Theory and Applications. Wiley.
15. Bhatti, F. A., Hamedani, G. G., Korkmaz, M. Ç., Yousof, H. M., & Ahmad, M. (2023). On The New Modified Burr XII Distribution: Development, Properties, Characterizations and Applications. Pakistan Journal of Statistics and Operation Research, 19(2), 327-348.
16. Bryson, M. C. (1974). Heavy-tailed distribution: properties and tests, Technimetrics, 16, 161-68.
17. Chahkandi, M. and Ganjali, M. (2009). On some lifetime distributions with decreasing failure rates, Computational Statistics and Data Analysis 53, 4433-4440.
18. Chesneau, C. and Yousof, H. M. (2021). On a special generalized mixture class of probabilistic models. Journal of Nonlinear Modeling and Analysis, 3(1), 71-92.
19. Cordeiro, G. M., Yousof, H. M., Ramires, T. G. and Ortega, E. M. M. (2018). The Burr XII system of densities: properties, regression model and applications. Journal of Statistical Computation and Simulation, 88(3), 432-456.
20. Durbey, S. D. (1970). Compound gamma, beta and F distributions, Metrika 16, 27-31.
21. Elbatal, I., Diab, L. S., Ghorbal, A. B., Yousof, H. M., Elgarhy, M., & Ali, E. I. (2024). A new losses (revenues) probability model with entropy analysis, applications and case studies for value-at-risk modeling and mean of order-P analysis. AIMS Mathematics, 9(3), 7169-7211.
22. Elgohari, H. and Yousof, H. M. (2020a). A Generalization of Lomax Distribution with Properties, Copula and Real Data Applications. Pakistan Journal of Statistics and Operation Research, 16(4), 697-711. https://doi.org/10.18187/pjsor.v16i4.3260
23. Elgohari, H. and Yousof, H. M. (2021b). A New Extreme Value Model with Different Copula, Statistical Properties and Applications. Pakistan Journal of Statistics and Operation Research, 17(4), 1015-1035. https://doi.org/10.18187/pjsor.v17i4.3471
24. Elgohari, H. and Yousof, H. M. (2020c). New Extension of Weibull Distribution: Copula, Mathematical Properties and Data Modeling. Statistics, Optimization & Information Computing, 8(4), 972-993. https://doi.org/10.19139/soic-2310-5070-1036
25. Elgohari, H., Ibrahim, M. and Yousof, H. M. (2021). A New Probability Distribution for Modeling Failure and Service Times: Properties, Copulas and Various Estimation Methods. Statistics, Optimization & Information Computing, 8(3), 555-586.
26. El-Morshedy, M., Alshammari, F. S., Hamed, Y. S., Eliwa, M. S., & Yousof, H. M. (2021). A new family of continuous probability distributions. Entropy, 23(2), 194.
27. Embrechts, P., Klüppelberg, C., & Mikosch, T. (2013). Modelling Extremal Events: For Insurance and Finance (2nd ed.). Springer.
28. Elsayed, H. A., & Yousof, H. M. (2019a). A new Lomax distribution for modeling survival times and taxes revenue data sets. Journal of Statistics and Applications, 2(1), 35-58.
29. Elsayed, H. A. H. and Yousof, H. M. (2019b). The Burr X Nadarajah Haghighi distribution: statistical properties and application to the exceedances of flood peaks data. Journal of Mathematics and Statistics, 15, 146-157.
30. Elsayed, H. A. H., & Yousof, H. M. (2020). The generalized odd generalized exponential Fréchet model: univariate, bivariate and multivariate extensions with properties and applications to the univariate version. Pakistan Journal of Statistics and Operation Research, 529-544.
31. Elsayed, H. A. H. and Yousof, H. M. (2021). Extended Poisson Generalized Burr XII Distribution. Journal of Applied Probability and Statistics, 16(1), 01-30.
32. Gupta, R. C., Gupta, P. L. and Gupta, R. D. (1998). Modeling failure time data by Lehman alternatives. Communications in Statistics-Theory and methods, 27(4), 887-904.
33. Corbellini, A., Crosato, L., Ganugi, P and Mazzoli, M. (2007). Fitting Pareto II distributions on firm size: Statistical methodology and economic puzzles. Paper presented at the International Conference on Applied

Stochastic Models and Data Analysis, Chania, Crete.
34. Cordeiro, G. M., Ortega, E. M. and Popovic, B. V. (2015). The gamma-Lomax distribution. Journal of Statistical computation and Simulation, 85(2), 305-319.
35. Elbiely, M. M., & Yousof, H. M. (2018). A new extension of the Lomax distribution and its applications. J. Stat. Appl, 2, 18-34.
36. Elbiely, M. M., & Yousof, H. M. (2019a). A new flexible Weibull Burr XII distribution. Journal of Statistics and Applications, 2(1), 59-77.
37. Elbiely, M. M. and Yousof, H. M. (2019b). A New Inverse Weibull Distribution: Properties and Applications. Journal of Mathematics and Statistics, 15(1), 30-43.
38. Emam, W.; Tashkandy, Y.; Hamedani, G.G.; Shehab, M.A.; Ibrahim, M.; Yousof, H.M. (2023a). A Novel Discrete Generator with Modeling Engineering, Agricultural and Medical Count and Zero-Inflated Real Data with Bayesian, and Non-Bayesian Inference. Mathematics 2023, 11, 1125. https://doi.org/10.3390/math110511.
39. Emam, W.; Tashkandy, Y.; Goual, H.; Hamida, T.; Hiba, A.; Ali, M.M.; Yousof, H.M.; Ibrahim, M. (2023b). A New One-Parameter Distribution for Right Censored Bayesian and Non-Bayesian Distributional Validation under Various Estimation Methods. Mathematics 2023, 11, 897. https://doi.org/10.3390/math1104089
40. Harris, C.M. (1968). The Pareto distribution as a queue service descipline, Operations Research, 16, 307-313.
41. Hashem, A. F., Abdelkawy, M. A., Muse, A. H., & Yousof, H. M. (2024). A novel generalized Weibull Poisson G class of continuous probabilistic distributions with some copulas, properties and applications to real-life datasets. Scientific Reports, 14(1), 1741.
42. Hashempour, M., Alizadeh, M., & Yousof, H. M. (2023). A New Lindley Extension: Estimation, Risk Assessment and Analysis Under Bimodal Right Skewed Precipitation Data. Annals of Data Science, 1-40.
43. Hosking, J. R. M., & Wallis, J. R. (1987). Parameter and quantile estimation for the generalized Pareto distribution. Technometrics, 29(3), 339-349.
44. Ibrahim, M. and Yousof, H. M. (2020). A new generalized Lomax model: statistical properties and applications, Journal of Data Science, 18(1), 190 - 217.
45. Ibrahim, M. (2019). A new extended Fréchet distribution: properties and estimation. Pak. J. Stat. Oper. Res.,15 (3), 773-796.
46. Ibrahim, M. (2020a). The compound Poisson Rayleigh Burr XII distribution: properties and applications. Journal of Applied Probability and Statistics, 15(1), 73-97.
47. Ibrahim, M. (2020b). The generalized odd Log-logistic Nadarajah Haghighi distribution: statistical properties and different methods of estimation. J. Appl. Probab. Stat, 15, 61-84.
48. Ibrahim, M., Yadav, A. S., Yousof, H. M., Goual, H. and Hamedani, G. G. (2019). A new extension of Lindley distribution: modified validation test, characterizations and different methods of estimation. Communications for Statistical Applications and Methods, 26(5), 473-495.
49. Jansen, D., & de Vries, C. G. (1991). On the frequency of large stock returns: Putting booms and busts into perspective. The Review of Economics and Statistics, 73(1), 18-24.
50. Lemonte, A. J. and Cordeiro, G. M. (2013). An extended Lomax distribution. Statistics, 47(4), 800-816.
51. Lomax, K.S. (1954). Business failures: Another example of the analysis of failure data, Journal of the American Statistical Association, 49, 847-852.
52. Gad, A. M., Hamedani, G. G., Salehabadi, S. M. and Yousof, H. M. (2019). The Burr XII-Burr XII distribution: mathematical properties and characterizations. Pakistan Journal of Statistics, 35(3), 229-248.
53. Ghosh, I. and Ray. S. (2016). Some alternative bivariate Kumaraswamy type distributions via copula with application in risk management. Journal of Statistical Theory and Practice 10, 693-706.
54. Gleaton, J. U. and Lynch, J.D. (2006). Properties of generalized loglogistic families of lifetime distributions. Journal of Probability and Statistical Science, 4, 51-64.
55. Goual, H. and Yousof, H. M. (2020). Validation of Burr XII inverse Rayleigh model via a modified chi-squared goodness-of-fit test. Journal of Applied Statistics, 47(3), 393-423.
56. Goual, H., Yousof, H. M. and Ali, M. M. (2019). Validation of the odd Lindley exponentiated exponential by a modified goodness of fit test with applications to censored and complete data. Pakistan Journal of Statistics an Operation Research, 15(3), 745-771.
57. Goual, H., Yousof, H. M. and Ali, M. M. (2020). Lomax inverse Weibull model: properties, applications and a modified Chi-squared goodness-of-fit test for validation, Journal of Nonlinear Science and Applications. 13(6), 330-353.
58. Gumbel, E. J. (1961). Bivariate logistic distributions. Journal of the American Statistical Association, 56(294), 335-349.
59. Gumbel, E. J. (1960) Bivariate exponential distributions. Journ. Amer. Statist. Assoc., 55, 698-707.

60. Hashem, A. F., Alotaibi, N., Alyami, S. A., Abdelkawy, M. A., Elgawad, M. A. A., Yousof, H. M., & Abdel-Hamid, A. H. (2024). Utilizing Bayesian inference in accelerated testing models under constant stress via ordered ranked set sampling and hybrid censoring with practical validation. Scientific Reports, 14(1), 14406.
61. Hamedani, G. G., Goual, H., Emam, W., Tashkandy, Y., Ahmad Bhatti, F., Ibrahim, M. and Yousof, H. M. (2023). A new right-skewed one-parameter distribution with mathematical characterizations, distributional validation, and actuarial risk analysis, with applications. Symmetry, 15(7), 1297.
62. Klugman, S. A., Panjer, H. H., & Willmot, G. E. (2012). Loss Models: From Data to Decisions (4th ed.). Wiley.
63. Korkmaz, M. C., Altun, E., Chesneau, C., & Yousof, H. M. (2022). On the unit-Chen distribution with associated quantile regression and applications. Mathematica Slovaca, 72(3), 765-786.
64. Korkmaz, M. Ç., Cordeiro, G. M., Yousof, H. M., Pescim, R. R., Afify, A. Z., & Nadarajah, S. (2019). The Weibull Marshall–Olkin family: Regression model and application to censored data. Communications in Statistics-Theory and Methods, 48(16), 4171-4194.
65. Korkmaz, M. Ç., Yousof, H. M., & Ali, M. M. (2017). Some theoretical and computational aspects of the odd Lindley Fréchet distribution. İstatistikçiler Dergisi: İstatistik ve Aktüerya, 10(2), 129-140.
66. Kotz, S. and Johnson, N. L. (1992). Breakthroughs in Statistics: Foundations and basic theory. Springer,Volume 1.
67. Loubna, H., Goual, H., Alghamdi, F. M., Mustafa, M. S., Tekle Mekiso, G., Ali, M. M., ... & Yousof, H. M. (2024). The quasi-xgamma frailty model with survival analysis under heterogeneity problem, validation testing, and risk analysis for emergency care data. Scientific Reports, 14(1), 8973.
68. Mansour, M. M., Butt, N. S., Yousof, H., Ansari, S. I., & Ibrahim, M. (2020a). A generalization of reciprocal exponential model: clayton copula, statistical properties and modeling skewed and symmetric real data sets. Pakistan Journal of Statistics and Operation Research, 373-386.
69. Mansour, M. M., Ibrahim, M., Aidi, K., Shafique Butt, N., Ali, M. M., Yousof, H. M. and Hamed, M. S. (2020b). A New Log-Logistic Lifetime Model with Mathematical Properties, Copula, Modified Goodness-of-Fit Test for Validation and Real Data Modeling. Mathematics, 8(9), 1508.
70. Mansour, M., Korkmaz, M. Ç., Ali, M. M., Yousof, H., Ansari, S. I., & Ibrahim, M. (2020c). A generalization of the exponentiated Weibull model with properties, Copula and application. Eurasian Bulletin of Mathematics (ISSN: 2687-5632), 3(2), 84-102.
71. Mansour, M., Rasekhi, M., Ibrahim, M., Aidi, K., Yousof, H. M. and Elrazik, E. A. (2020d). A New Parametric Life Distribution with Modified Bagdonavičius-Nikulin Goodness-of-Fit Test for Censored Validation, Properties, Applications, and Different Estimation Methods. Entropy, 22(5), 592.
72. Mansour, M., Yousof, H. M., Shehata, W. A. M. and Ibrahim, M. (2020e). A new two parameter Burr XII distribution: properties,copula, different estimation methods and modeling acute bone cancer data, Journal of Nonlinear Science and Applications, 13, 223-238.
73. McNeil, A. J., Frey, R., & Embrechts, P. (2015). Quantitative Risk Management: Concepts, Techniques, and Tools. Princeton University Press.
74. Mohamed, H. S., Cordeiro, G. M., Minkah, R., Yousof, H. M., & Ibrahim, M. (2024). A size-of-loss model for the negatively skewed insurance claims data: applications, risk analysis using different methods and statistical forecasting. Journal of Applied Statistics, 51(2), 348-369.
75. Morgenstern, D. (1956). Einfache beispiele zweidimensionaler verteilungen. Mitteilingsblatt fur Mathematische Statistik, 8, 234-235.
76. Murthy, D.N.P. Xie, M. and Jiang, R. (2004). Weibull Models, Wiley.
77. Nasir, M. A., Korkmaz, M. C., Jamal, F. and Yousof, H. M. (2018). On a new Weibull Burr XII distribution for lifetime data. Sohag Journal of Mathematics, 5(2), 47-56.
78. Nofal, Z. M., Afify, A. Z., Yousof, H. M., Granzotto, D. C., & Louzada, F. (2016). Kumaraswamy transmuted exponentiated additive Weibull distribution. International Journal of Statistics and Probability, 5(2), 78-99.
79. Pougaza, D. B. and Djafari, M. A. (2011). Maximum entropies copulas. Proceedings of the 30th international workshop on Bayesian inference and maximum Entropy methods in Science and Engineering, 329-336.
80. Poon, S. H., & Rockinger, M. (2003). The conditional distribution of extreme stock market returns: An empirical analysis. Journal of Empirical Finance, 10(4), 373-400.
81. Rasekhi, M., Altun, E., Alizadeh, M. and Yousof, H. M. (2022). The Odd Log-Logistic Weibull-G Family of Distributions with Regression and Financial Risk Models. Journal of the Operations Research Society of China, 10(1), 133-158.
82. Rasekhi, M., Saber, M. M., & Yousof, H. M. (2020). Bayesian and classical inference of reliability in multicomponent stress-strength under the generalized logistic model. Communications in Statistics-Theory and Methods, 50(21), 5114-5125.

83. Rodriguez-Lallena, J. A. and Ubeda-Flores, M. (2004). A new class of bivariate copulas. Statistics and Probability Letters, 66, 315-25.
84. Salem, M., Emam, W., Tashkandy, Y., Ibrahim, M., Ali, M. M., Goual, H., & Yousof, H. M. (2023). A new lomax extension: Properties, risk analysis, censored and complete goodness-of-fit validation testing under left-skewed insurance, reliability and medical data. Symmetry, 15(7), 1356.
85. Shehata, W. A., Goual, H., Hamida, T., Hiba, A., Hamedani, G. G., Al-Nefaie, A. H., ... & Yousof, H. M. (2024). Censored and Uncensored Nikulin-Rao-Robson Distributional Validation: Characterizations, Classical and Bayesian estimation with Censored and Uncensored Applications. Pakistan Journal of Statistics and Operation Research, 11-35.
86. Shrahili, M.; Elbatal, I. and Yousof, H. M. Asymmetric Density for Risk Claim-Size Data: Prediction and Bimodal Data Applications. Symmetry 2021, 13, 2357. https://doi.org/10.3390/sym13122357
87. Teghri, S., Goual, H., Loubna, H., Butt, N. S., Khedr, A. M., Yousof, H. M., ... & Salem, M. (2024). A New Two-Parameters Lindley-Frailty Model: Censored and Uncensored Schemes under Different Baseline Models: Applications, Assessments, Censored and Uncensored Validation Testing. Pakistan Journal of Statistics and Operation Research, 109-138.
88. Reynkens, T., Verbelen, R., Beirlant, J., & Antonio, K. (2017). Modelling censored losses using splicing: A global fit strategy with mixed Erlang and extreme value distributions. Insurance: Mathematics and Economics, 77, 65-77.
89. Tahir, M. H., Cordeiro, G. M., Mansoor, M., & Zubair, M. (2015). The Weibull-Lomax distribution: properties and applications. Hacettepe Journal of Mathematics and Statistics, 44(2), 461-480.
90. Yadav, A.S., Goual, H., Alotaibi, R.M. Rezk, H., Ali, M.M. and Yousof, H.M. (2020). Validation of the Topp-Leone-Lomax model via a modified Rao-Robson-Nikulin goodness-of-fit test with different methods of estimation. Symmetry, 12, 1-26. doi: 10.3390/sym12010057
91. Yousof, H. M., Afify, A. Z., Abd El Hadi, N. E., Hamedani, G. G., & Butt, N. S. (2016). On six-parameter Fréchet distribution: properties and applications. Pakistan Journal of Statistics and Operation Research, 281-299.
92. Yousof, H. M., Altun, E., & Hamedani, G. G. (2018). A NEW EXTENSION OF FRÉCHET DISTRIBUTION WITH REGRESSION MODELS, RESIDUAL ANALYSIS AND CHARACTERIZATIONS. Journal of Data Science, 16(4).
93. Yousof, H. M., Ahsanullah, M. and Khalil, M. G. (2019). A New Zero-Truncated Version of the Poisson Burr XII Distribution: Characterizations and Properties. Journal of Statistical Theory and Applications, 18(1), 1-11.
94. Yousof, H. M., Alizadeh, M., Jahanshahi and, S. M. A., Ramires, T. G., Ghosh, I. and Hamedani, G. G. (2017). The Topp-Leone Transmuted G family of distributions: theory, characterizations and applications. Journal of Data Science, 15(4), 723-740.
95. Yousof, H. M., Korkmaz, M. Ç., K., Hamedani, G. G and Ibrahim, M. (2022). A novel Chen extension: theory, characterizations and different estimation methods. Eur. J. Stat, 2(2022), 1-20.
96. Yousof, H. M., Altun, E., Ramires, T. G., Alizadeh, M. and Rasekhi, M. (2018). A new family of distributions with properties, regression models and applications, Journal of Statistics and Management Systems, 21, 1, 163-188.
97. Yousof, H. M., Ansari, S. I., Tashkandy, Y., Emam, W., Ali, M. M., Ibrahim, M., Alkhayyat, S. L. (2023a). Risk Analysis and Estimation of a Bimodal Heavy-Tailed Burr XII Model in Insurance Data: Exploring Multiple Methods and Applications. Mathematics. 2023; 11(9):2179. https://doi.org/10.3390/math11092179
98. Yousof, H. M., Goual, H., Khaoula, M. K., Hamedani, G. G., Al-Aefaie, A. H., Ibrahim, M., ... & Salem, M. (2023b). A Novel Accelerated Failure Time Model: Characterizations, Validation Testing, Different Estimation Methods and Applications in Engineering and Medicine. Pakistan Journal of Statistics and Operation Research, 691-717.
99. Yousof, H. M., Majumder, M., Jahanshahi, S. M. A., Ali, M. M. and Hamedani G. G. (2018). A new Weibull class of distributions: theory, characterizations and applications, Journal of Statistical Research of Iran, 15, 45-83.
100. Yousof, H. M., Saber, M. M., Al-Nefaie, A. H., Butt, N. S., Ibrahim, M., & Alkhayyat, S. L. (2024). A discrete claims-model for the inflated and over-dispersed automobile claims frequencies data: Applications and actuarial risk analysis. Pakistan Journal of Statistics and Operation Research, 261-284.
101. Yousof, H.M.; Tashkandy, Y.; Emam, W.; Ali, M.M.; Ibrahim, M. (2023c). A New Reciprocal Weibull Extension for Modeling Extreme Values with Risk Analysis under Insurance Data. Mathematics 2023, 11, 966. https://doi.org/10.3390/ math11040966